

Rockefeller University

Digital Commons @ RU

---

Student Theses and Dissertations

---

1971

## Field Theoretic Models of Deep Inelastic Lepton-Nucleon Scattering

Stephen Blaha

Follow this and additional works at: [https://digitalcommons.rockefeller.edu/student\\_theses\\_and\\_dissertations](https://digitalcommons.rockefeller.edu/student_theses_and_dissertations)



Part of the [Life Sciences Commons](#)

---

FIELD THEORETIC MODELS OF DEEP INELASTIC  
LEPTON-NUCLEON SCATTERING

A thesis submitted to the Faculty of The Rockefeller University  
in partial fulfillment of the requirements  
for the degree of Doctor of Philosophy

by

Stephen Blaha, B.S.

APPROVED FOR PUBLICATION

A handwritten signature in black ink, appearing to read 'M.A.B. Bég', with a stylized flourish at the end.

M.A.B. Bég  
Professor

19 April 1971  
The Rockefeller University  
New York





## PREFACE

It is a pleasure to thank my advisor, Professor M.A.B.Beg, for his advice and instruction during my graduate work. His pointed critiques and helpful suggestions have played an important role in my education.

In addition I would like to thank the other members of the Physics Department, and in particular, Professors Pais, Khuri and Pagels, for their contributions to my development as a physicist.

I am grateful to Miss Judy Cuzzo for the diligence and skill she displayed in typing this thesis.

## SUMMARY

We investigate the asymptotic behavior of the inelastic electron-nucleon structure functions within the framework of ladder models of the virtual Compton amplitude in the limit  $|q^2| \rightarrow \infty$  with  $\omega = 2q \cdot p / |q^2|$  large and fixed. ( $q$  is the electron four-momentum transfer and  $p$  the target nucleon momentum.) The leading logarithmic behavior of the ladder diagrams is obtained by Mellin transform techniques. Our results are:

1. The structure functions do not scale (i.e. become non-trivial functions of  $\omega$ ) in our neutral vector meson ladder model and our pseudoscalar meson model because of the appearance of factors of  $\ln|q^2|$ . We also find the neutrino-nucleon structure functions in analogous ladder models and they exhibit the same non-scaling behavior. In all cases  $\nu W_2$ ,  $W_1$  and  $\nu W_3$  (in the case of neutrino scattering) diverge as  $|q^2| \rightarrow \infty$ .

2. In a truss bridge diagram model similar to that of Bjorken and Wu  $\nu W_2$  scales while  $W_1$  does not.

3. To fourth order in the meson-nucleon coupling constant,  $g$ , ladder diagrams are the only Compton scattering diagrams contributing to the leading logarithm for each order in  $g$  in the neutral vector meson theory and pseudoscalar meson theory. Ladder diagrams with nucleon loops contribute to the leading logarithm in the neutral vector meson theory but do not contribute to the leading logarithm in the pseudoscalar meson theory.

4. The leading part of the Bethe-Salpeter for the Compton amplitude in the neutral vector meson ladder model is closely related to Jackiw's Bethe-Salpeter equation for the electromagnetic vertex. ( $MT_\mu^{\mu}$  which is the trace of the spin-averaged virtual Compton amplitude is equal to Jackiw's off-mass-shell solution for the vertex where  $M$  is the nucleon mass.)

## TABLE OF CONTENTS

## CHAPTER

I.	INTRODUCTION . . . . .	1
	A. The Experimental Situation . . . . .	1
	B. Technical Introduction . . . . .	3
	C. Ladder Models of the Forward Virtual Compton Amplitude . . . . .	9
II.	"SCALAR NUCLEON" MODELS . . . . .	14
	A. General Form of the (N+1) Rung Ladder Diagram . . . . .	14
	B. The "Scalar Photon, Nucleon and Meson" Model . . . . .	19
	C. The Vector Photon, "Scalar Nucleon" and Scalar Meson Model . . . . .	23
III.	SPIN ONE-HALF NUCLEON MODELS . . . . .	30
	A. Introduction . . . . .	30
	B. The Neutral Vector Meson Model . . . . .	31
	C. The Neutral Pseudoscalar Meson Model . . . . .	47
	D. A Truss Bridge Diagram Model . . . . .	48
IV.	COMMENTS ON THE SPIN ONE-HALF NUCLEON MODELS . . . . .	55
	A. The Leading Behavior of Non-Ladder Diagrams . . . . .	55
	B. The Bethe-Salpeter Equations For the Neutral Vector Meson Model of the Virtual Compton Amplitude and its Relation to Jackiw's Bethe-Salpeter Equation For the Vertex . . . . .	70

C. Comparison With Experiment . . . . .	75
D. Neutrino-Nucleon Scattering . . . . .	78
APPENDICES . . . . .	82
A. THE SPINOR POLYNOMIALS . . . . .	82
B. THE FEYNMAN PARAMETER POLYNOMIALS, C AND D .	87
C. THE DERIVATIVES OF $\exp[iD(A)/C]$ . . . . .	92
BIBLIOGRAPHY . . . . .	101

## CHAPTER I

### Introduction

#### A. The Experimental Situation

This thesis describes investigations of deep inelastic electron-nucleon scattering in several field theoretic models. The current interest in this topic was based on the point-like nature of the electron which enabled experimenters to directly probe the electromagnetic structure of the nucleon.

Thus experimenters and theorists spoke of "seeing" the electromagnetic structure of the nucleons in electron-nucleon scattering experiments. The interest in deep inelastic scattering was further stimulated by the striking form of the initial experimental data of Bloom et al.<sup>1</sup> In order to describe the data it will first be necessary to define the kinematics of the experiment.

The typical experiment consists of an electron scattering off a nucleon and producing a final state consisting of an electron and a collection of other particles, denoted by  $n$ . The initial and final electron four-momenta are  $k$  and  $k'$  respectively. The initial nucleon momentum is  $p$ , and the total momentum of the particles,  $n$ , is  $p_n$ .

Quantum electrodynamics suggests that the scattering event is well described by an electron-nucleon interaction consisting of the exchange of a virtual photon of momentum,  $q=k-k'$ . Fig. (I.1) depicts the scattering. It is possible that scattering through the exchange of several virtual photons may not be negligible (especially in light of the work by Brodsky et al.<sup>2</sup>). We assume the one virtual photon exchange process is dominant.

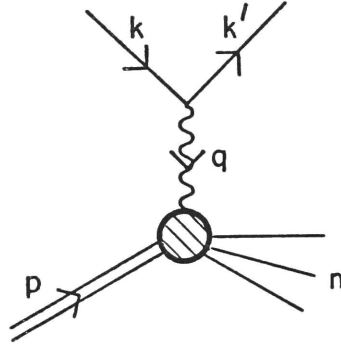


Fig. I.1 Electron-Nucleon Scattering via One Photon Exchange.

In the initial experiment of Bloom et al.<sup>1</sup> the incoming electron energy  $E$ , the outgoing electron energy  $E'$ , and the electron scattering angle  $\theta$  were measured in the laboratory reference frame. The differential cross-section for this experiment is<sup>3</sup> (cf. section (Ib)):

$$\frac{d\sigma}{d\Omega dE'} = \frac{\alpha^2}{4E^2 \sin^4(\frac{\theta}{2})} [2 W_1 \sin^2(\frac{\theta}{2}) + W_2 \cos^2(\frac{\theta}{2})] \quad (\text{I.1})$$

where  $\alpha$  is the fine structure constant and the electron mass is negligible compared to  $E$  and  $E'$ .  $W_1$  and  $W_2$  are functions resulting from the nucleon's complex structure and are thus called the nucleon inelastic structure functions. Lorentz and gauge invariance require that there be only two functions (cf. section (I.b)) and that they be functions of two variables,  $q^2$  and  $\nu = q \cdot p / M$  where  $M$  is the nucleon mass. In terms of the electron variables  $\nu$  and  $q^2$  are given by

$$\begin{aligned} \nu &= E - E' \\ q^2 &= -4E E' \sin^2(\frac{\theta}{2}) \end{aligned} \quad (\text{I.2})$$

where the electron mass is neglected in comparison to  $E$  and  $E'$  in the  $q^2$  equation.

Bloom et al's <sup>1</sup> electron-proton scattering data suggested that the proton structure function,  $W_{2p}$ , has a particularly simple form in the deep inelastic region where  $|q^2|$  and  $q.p$  are of order of  $1(\text{GeV})$ .<sup>2</sup> Rather than being a function of two variables  $vW_{2p}$  is only a function of one variable,  $\omega=2Mv/|q^2|$ . This behavior is called scaling and it was predicted by Bjorken <sup>4</sup> prior to the experiment. Because of scaling  $vW_2$  can be represented by the two dimensional plot in Fig. (I.2). Recently the neutron's structure function has also been found to scale (Bloom et al.). In this thesis we will calculate  $W_1$  and  $W_2$  in several field theory models in an attempt to understand the origin of scaling and other aspects of the experimental data.

## B. Technical Introduction

In this section we describe the derivation of eq. (I.1) and relate the inelastic structure functions to the forward virtual Compton amplitude.

The invariant amplitude corresponding to the scattering diagram Fig. (I.1) is

$$\mathcal{M} = -e^2 \bar{u}(k') \gamma^\mu u(k) \frac{1}{q^2} \langle n | J_\mu | p \rangle \quad (\text{I.3})$$

where  $e$  is the electron charge,  $u(k)$  is a Dirac spinor ( we follow the conventions of Bjorken and Drell<sup>5</sup> ) and  $\langle n | J_\mu | p \rangle$  is the matrix element of the hadronic electromagnetic current



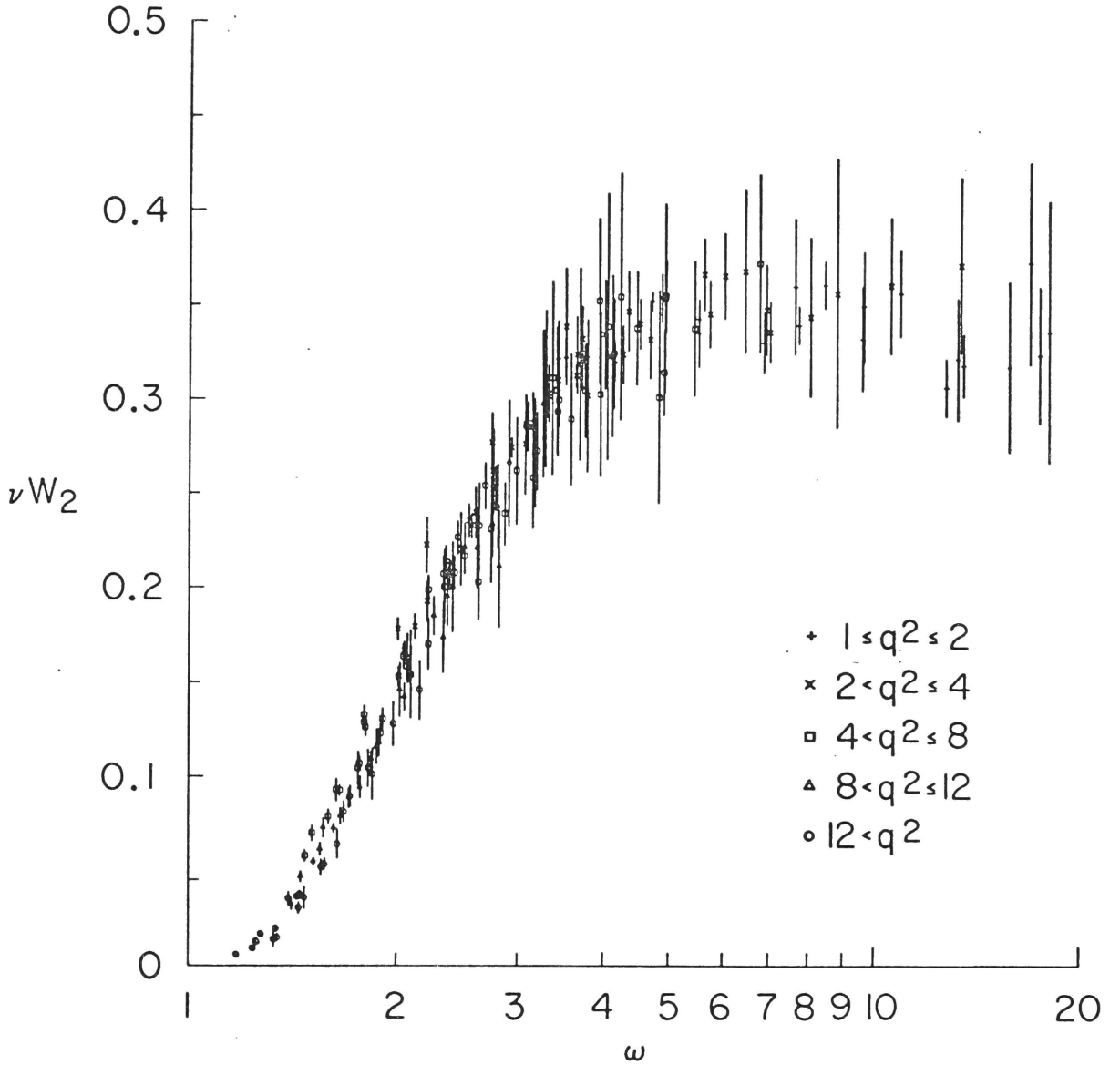


Fig. I.2.  $\nu W_2$  versus  $\omega$  for  $(p+q)^2 > 4(\text{GeV})^2$  and  $|q^2| > 1(\text{GeV})^2$  assuming  $\omega \nu W_2 = 2.36 M W_1$  as suggested by experiment.

between the incident nucleon state,  $|p\rangle$ , and the final hadronic state  $|n\rangle$ . It is normalized so that

$$\langle n | J_\mu | p \rangle = -i \bar{u}(p_n) \gamma_\mu u(p) \quad (\text{I.4})$$

for a point-like incident nucleon.

In the experiment of Bloom et al. no attempt was made to measure spins or detect any special final hadronic state. Consequently the cross-section is given by

$$d\sigma = \frac{2\alpha^2 M d^3 k'}{E' \sqrt{(k \cdot p)^2 - m^2 M^2}} [k'_\mu k'_\nu + k'_\nu k'_\mu - g_{\mu\nu} (k \cdot k' - m^2)] W^{\mu\nu} \quad (\text{I.5})$$

where  $m$  is the electron's mass and

$$W_{\mu\nu} = \sum_n (2\pi)^3 \delta^4(q + p - p_n) \langle p | J_\mu | n \rangle \langle n | J_\nu | p \rangle \quad (\text{I.6})$$

Below we will show that  $W_{\mu\nu}$  can be put in the form

$$W_{\mu\nu} = -(g_{\mu\nu} - \frac{q_\mu q_\nu}{q^2}) W_1 + \frac{1}{M^2} (p_\mu - \frac{q \cdot p}{q^2} q_\mu) (p_\nu - \frac{q \cdot p}{q^2} q_\nu) W_2 \quad (\text{I.7})$$

Eq. (I.1) is obtained if we evaluate  $d\sigma$  in the laboratory reference frame and use eq. (I.7) in eq. (I.5). The electron mass is treated as negligible in comparison to  $E$  and  $E'$ .

We now show that Lorentz and gauge invariance imply  $W_{\mu\nu}$  can be put in the form of eq. (I.7). It is clear from eq. (I.6) that  $W_{\mu\nu}$  is a second rank Lorentz tensor which is a function only of the four vectors  $q$  and  $p$ . Since the nucleon is spin-averaged the most general form of  $W_{\mu\nu}$  is

$$W_{\mu\nu} = A p_\mu p_\nu + B p_\nu q_\mu + C p_\mu q_\nu + D q_\mu q_\nu + E g_{\mu\nu} \quad (I.8)$$

where A,B,C,D and E are Lorentz scalar functions of  $q^2, q \cdot p$  and  $p^2=M^2$ . Gauge invariance implies

$$q^\mu W_{\mu\nu} = 0 \quad (I.9a)$$

$$q^\nu W_{\mu\nu} = 0 \quad (I.9b)$$

Eqs. (I.8) and (I.9a) lead to

$$q \cdot p A + q^2 B = 0 \quad (I.10a)$$

$$q \cdot p C + q^2 D + E = 0 \quad (I.10b)$$

if we remember that  $q$  and  $p$  are independent variables and thus the coefficients of  $p_\nu$  and  $q_\nu$  must vanish separately for eq. (I.9a) to hold. Similarly eq. (I.9b) results in another constraint on the scalar functions:

$$A q \cdot p + C q^2 = 0 \quad (I.10c)$$

The second constraint on the scalar functions implied by eq. (I.9b) is not independent of those already given in eqs. (I.10).

As a consequence of eqs. (I.10)  $W_{\mu\nu}$  may be written

$$W_{\mu\nu} = A p_\mu p_\nu - A \frac{q \cdot p}{q^2} (q_\mu p_\nu + q_\nu p_\mu) + D q_\mu q_\nu - (q^2 D - \frac{(q \cdot p)^2}{q^2} A) g_{\mu\nu} \quad (I.11)$$

If we now define  $A = M^{-2} W_2$  and  $W_1 = q^2 D - \frac{(q \cdot p)^2}{q^2} A$  then eq. (I.11) becomes eq. (I.7).

The inelastic structure functions are related to the imaginary part of the forward virtual Compton amplitude. The forward Compton amplitude corresponding to Fig. (I.3)

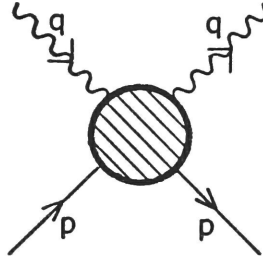


Fig. I.3. The Forward Compton Amplitude Diagram

is

$$T = N \epsilon_{\mu}^f \epsilon_{\nu}^i T^{\mu\nu} \quad (\text{I.12})$$

where  $N$  is a normalization factor,  $\epsilon^i$  is the polarization of the incoming and  $\epsilon^f$  of the outgoing photon, and

$$T_{\mu\nu} = i \int d^4z e^{iq \cdot z} \langle p | T^* (J_{\mu}(z) J_{\nu}(0)) | p \rangle \quad (\text{I.13})$$

with  $T^*$  the covariant time ordered product. From Lorentz and gauge invariance one can show

$$T_{\mu\nu} = -\left(g_{\mu\nu} - \frac{q_{\mu} q_{\nu}}{q^2}\right) T_1 + \frac{1}{M^2} \left(p_{\mu} - \frac{p \cdot q}{q^2} q_{\mu}\right) \left(p_{\nu} - \frac{p \cdot q}{q^2} q_{\nu}\right) T_2 \quad (\text{I.14})$$

in the same manner as eq. (I.7).

If we introduce a complete set of intermediate states  $|n\rangle$  into eq. (I.13), use the relation

$$\langle p | J_\alpha(z) | n \rangle = e^{i(p-p_n) \cdot z} \langle p | J_\alpha(0) | n \rangle$$

and perform the integrations over the  $z$  variables we obtain

$$T_{\mu\nu} = - \sum_n \frac{(2\pi)^3 \delta^{(3)}(\vec{p} + \vec{q} - \vec{p}_n)}{q_0 + p_0 - p_{n0} + ie} \{ \langle p | J_\mu(0) | n \rangle \langle n | J_\nu(0) | p \rangle - \langle p | J_\nu(0) | n \rangle \langle n | J_\mu(0) | p \rangle \}$$

where  $p_n$  is the total momentum of state  $n$  and  $p_{n0}$  is its total energy. We take the imaginary part of  $T_{\mu\nu}$  using the identity

$$\text{Im} \frac{1}{x+ie} = -\pi \delta(x)$$

and it is clear from eq. (I.6) that

$$W_{\mu\nu} = \frac{1}{\pi} \text{Im} T_{\mu\nu} \quad (\text{I.15})$$

In particular

$$W_1 = \frac{1}{\pi} \text{Im} T_1 \quad (\text{I.16a})$$

$$W_2 = \frac{1}{\pi} \text{Im} T_2 \quad (\text{I.16b})$$

Later we take advantage of these relationships by constructing models for the forward virtual Compton amplitude which give the inelastic structure functions upon taking the imaginary part.

### C. Ladder Models of the Forward Virtual Compton Amplitude

In this section we outline the models and procedures which will be used in subsequent chapters.

The first step in constructing a model is to choose a field theory which (hopefully) is related to the real world. Secondly, because of the extreme difficulty (if not impossibility) of computing the total contributions of all Feynman diagrams we only include ladder diagrams (Fig. (I.4)) in our model of the virtual Compton amplitude and approximate the contribution of each ladder diagram by its leading logarithm.

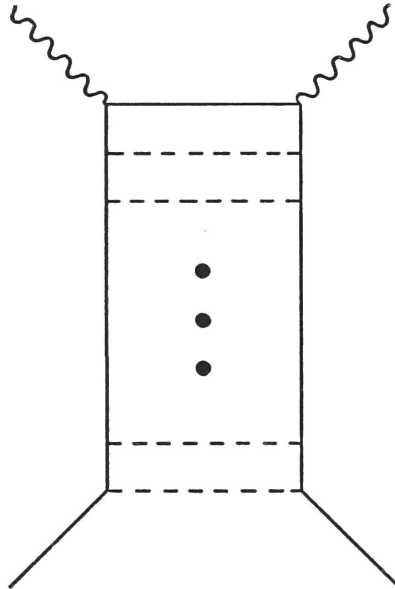


Fig. I.4. A Typical Ladder Diagram

As a result all other Feynman diagrams are ignored. There is no rigorous justification for ignoring these other diagrams. However, a partial justification can be given. In the region of the variables in which we are interested ( $|q^2| \rightarrow \infty$  with  $\omega$  fixed and large) the ladder diagram has a greater leading logarithmic behavior than any other diagram of the same order in the coupling constant (cf. Drell et al.,<sup>6</sup> Chang and Fishbane<sup>7</sup>, and section IV.A). This suggests that ladder diagrams may be the most important diagrams in the region of interest. Furthermore, the study of the set of ladder diagrams has been of heuristic value in the development of Regge theory and the multiperipheral model from a field theoretic viewpoint. Hopefully our investigation of ladder diagrams will reveal some features of a full field theoretic calculation.

Each ladder diagram corresponds to a multiple integral which is usually impossible to evaluate exactly. However it is possible to calculate the leading logarithmic term of the integral in any variable. To define the leading logarithmic term in a variable  $x$  we note that each term resulting from the Feynman integral can be put in the form  $Ax^r(\ln x)^s$  where  $A$ ,  $r$  and  $s$  are independent of  $x$ .

Let  $r_{\text{MAX}}$  be the maximum value of  $r$  occurring among the terms. Then the leading logarithmic term is the term which the largest  $s$  of all terms with  $r = r_{\text{MAX}}$ .

For each ladder diagram we compute the leading logarithmic term in  $|q^2|$  with  $\omega$  fixed. Then we assume  $\omega$  is large (though fixed) and find the leading logarithmic behavior in  $\omega$  of the coefficient of the leading logarithm in  $|q^2|$ . This limit

corresponds to the Regge region of the variables. It is also a region which has been probed by experiments.

Finally we sum the leading logarithms of the ladder graphs. The only justification for this procedure is the facility with which we are able to sum large classes of Feynman diagrams. However it should be remembered that lower order logarithmic terms might become important upon summing all ladder diagrams.<sup>8</sup> Indeed Wu<sup>8</sup> has given an example where the summation of leading terms does not agree with the exact solution. Therefore we should not expect any quantitative agreement of our results with experiment but we can hope to compare their qualitative features with experiment.

With these qualifications in mind we now state the structure functions which were calculated in the manner described above in various field theoretic ladder models. These results will be discussed in Chapter IV.

The first model of the type we have described was studied by Abarbanel et al<sup>9</sup> in 1969. In their model a "scalar" nucleon interacted with a scalar photon. The nucleon structure was induced by scalar mesons being exchanged on the rungs of ladder diagrams of the form of Fig. (I.4). Since the photon was treated as a scalar particle there was only one structure function which scaled when multiplied by  $q \cdot p$ :

$$q \cdot p W = \frac{c}{2} \omega^c \quad (I.17)$$

where  $c = g^2/16\pi^2 M^2$ ,  $g$  is the meson-nucleon coupling constant (cf. eq. (II.8)) and  $M$  is the nucleon mass. The calculation is performed in section IIB in order to illustrate our procedure.



Altarelli and Rubinstein<sup>10</sup> considered a model identical to Abarbanel et al's except that the photon was treated as a spin one particle. They found (cf. section IIC where we have outlined their calculation for the sake of completeness)

$$\nu W_2 = 2Mc\omega^{c-2} \quad (\text{I.18a})$$

$$M W_1 = 2M^3 c \frac{\ln|q^2|}{|q^2|} \omega^{c-1} \quad (\text{I.18b})$$

Drell et al<sup>11</sup> calculated the inelastic structure functions in a charged pseudo-scalar meson model with spin one photons and spin one-half nucleons. In addition they placed a cutoff,  $k_{\text{MAX}}$ , on the transverse momenta of the emitted pion at each pion-nucleon vertex. This was motivated by experimental data indicating that the transverse momenta in pion production is usually small. As a result they obtained scaling in both structure functions

$$\nu W_2 = \frac{1}{2} k a \omega^{a-1} \quad (\text{I.19a})$$

$$M W_1 = \frac{\omega}{2} \nu W_2 \quad (\text{I.19b})$$

for the neutron and proton with  $k$  a constant and

$$a = \frac{3g^2}{16\pi^2} \ln \left( 1 + \frac{k^2_{\text{MAX}}}{M^2} \right) \quad (\text{I.20})$$

In chapter III we calculate the behavior of the structure functions in a ladder model with spin one photons, spin one-half nucleons and neutral vector mesons (in the Feynman gauge) exchanged on the rungs of the ladder. Our results are (cf. section IIIB)

$$vW_2 = \frac{z}{\sqrt{2} \omega \ln \omega} I_1(\sqrt{2} z) \quad (\text{I.21a})$$

$$z = \frac{g}{2\pi} (\ln|q^2| \ln \omega)^{\frac{1}{2}} \quad (\text{I.21b})$$

where  $g$  is the meson-nucleon coupling constant and  $I_1(x)$  is a Bessel function<sup>12</sup>.  $W_1$  is related to  $W_2$  by eq. (I.19b).

It became apparent that the neutral vector meson model was closely related to a neutral pseudoscalar meson model which differed from Drell et al's model only in that no cutoff is placed on the transverse momenta of the mesons. The structure functions obtained in this model were (cf. section IIIC)

$$vW_2 = \frac{z}{2\omega \ln \omega} I_1(z) \quad (\text{I.22})$$

with  $z$  given in eq. (I.21b) and  $W_1$  related to  $W_2$  by eq. (I.19b).

Another model which is similar to the two immediately preceding models is a truss bridge diagram model (which is studied in section IIID). The structure functions in this model are

$$vW_2 = \frac{g^2}{M\pi G^2 \omega^2 \ln \omega} I_1(2\sigma^{\frac{1}{2}} \ln \omega) \quad (\text{I.23})$$

$$MW_1 = \frac{g^2 M}{\pi G^2 \omega |q^2|} \left( \frac{\ln|q^2|}{\ln \omega} \right)^{\frac{1}{2}} I_1(2(\sigma \ln|q^2| \ln \omega)^{\frac{1}{2}}) \quad (\text{I.24})$$

where  $\sigma = G/16\pi^2$ , and  $g$  and  $G$  are coupling constants defined in eq. (III.21).

## CHAPTER II

"Scalar Nucleon" Models

## A. General Form of the (N+1) Rung Ladder Diagram

The multiple integral corresponding to the (N+1) rung ladder diagram for virtual Compton Scattering (Fig. (I.4)) has a general form which is common to all the field theories we will be considering in this chapter and the next. We will develop the general form in this section. Then we will use it in succeeding sections to study models where the nucleon is treated as a scalar (spin 0) particle.

The contribution of the ladder diagram in Fig. (II.1) to the virtual Compton amplitude is denoted  $T_{N\mu\nu}$ .

To each line in Fig. (II.1) corresponds a Feynman propagator which is

$$\frac{i}{k^2 - M^2 + ie}$$

in the case of a spin 0 particle and is

$$\frac{i (\not{k} + M)}{k^2 - M^2 + ie}$$

for a spin one-half particle of four-momentum  $k$  and mass  $M$ .

Thus the Feynman integral corresponding to Fig. (II.1) may be

$$iT_{N\mu\nu} = \int \prod_{j=1}^N \frac{d^4 k_j}{(2\pi)^4} \frac{i^{3N+1} \mathcal{M}_{N\mu\nu}}{\prod_{j=1}^N (k_j^2 - M^2)^2 [(q+k_1)^2 - M^2] \prod_{r=1}^N [(k_{r+1} - k_r)^2 - m^2]} \quad (\text{II.1})$$

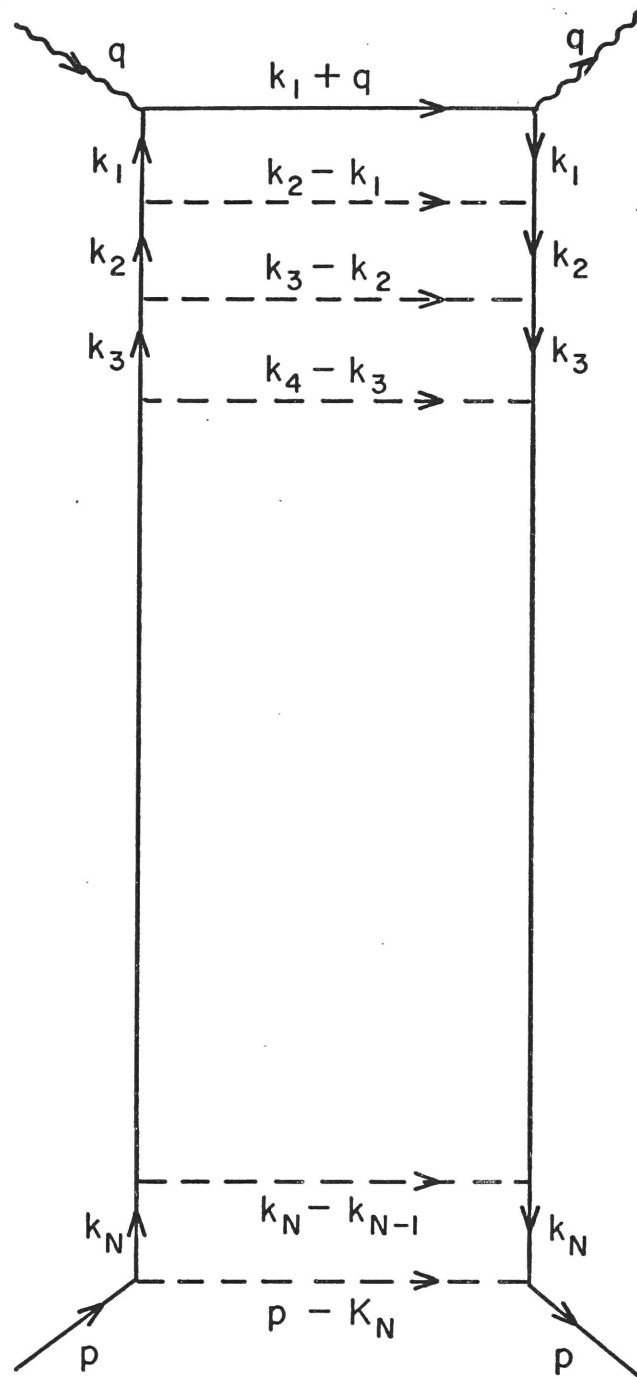


Fig. II.1  $(N+1)$  Rung Ladder Diagram

where  $m$  is the mass of particles corresponding to the dashed lines,  $M$  is the mass of particles corresponding to the solid lines and we let  $k_{N+1}=p$  for notational convenience. We have made the denominators and factor of  $i$  explicit for each particle propagator and lumped all other propagator and vertex factors into  $\mathcal{N}_{N\mu\nu}$ .  $\mathcal{N}_{N\mu\nu}$  is a polynomial in the loop momenta  $k_j$  for  $j=1,2,\dots,N$  in general.

In order to put eq. (II.1) in a more useful form we exponentiate each factor in the denominator through repeated use of the identity

$$\frac{1}{k^2 - M^2 + i\epsilon} = -i \int_0^\infty dz e^{iz(k^2 - M^2 + i\epsilon)} \quad (\epsilon > 0) \quad (\text{II.2})$$

where  $z$  is called a Feynman parameter. We label each line in the diagram with the Feynman parameter exponentiating the denominator factor in eq. (II.1) to which the line corresponded (Fig. (II.2)). As a result  $T_{N\mu\nu}$  becomes

$$iT_{N\mu\nu} = \int_0^\infty d\Omega \int \prod_j d^4k_j \frac{\mathcal{N}_{N\mu\nu}}{(2\pi)^{4N}} \exp(i\psi) \quad (\text{II.3})$$

with  $d\Omega = d\alpha_0 d\alpha_1 d\alpha_2 \dots d\alpha_N d\beta_1 \dots d\beta_N d\gamma_1 \dots d\gamma_N$  and

$$\psi = \alpha_0 [(q+k_1)^2 - M^2] + \sum_{j=1}^N \{ (\beta_j + \gamma_j) (k_j^2 - M^2) + \alpha_j [(k_{j+1} - k_j)^2 - m^2] \} \quad (\text{II.4})$$

If  $\mathcal{N}_{N\mu\nu}$  were independent of loop momenta the loop integrals in eq. (II.3) could be performed using standard techniques such as those described in Eden et al.<sup>13</sup> So we re-express the loop momenta dependence of terms in  $\mathcal{N}_{N\mu\nu}$  in a manner which

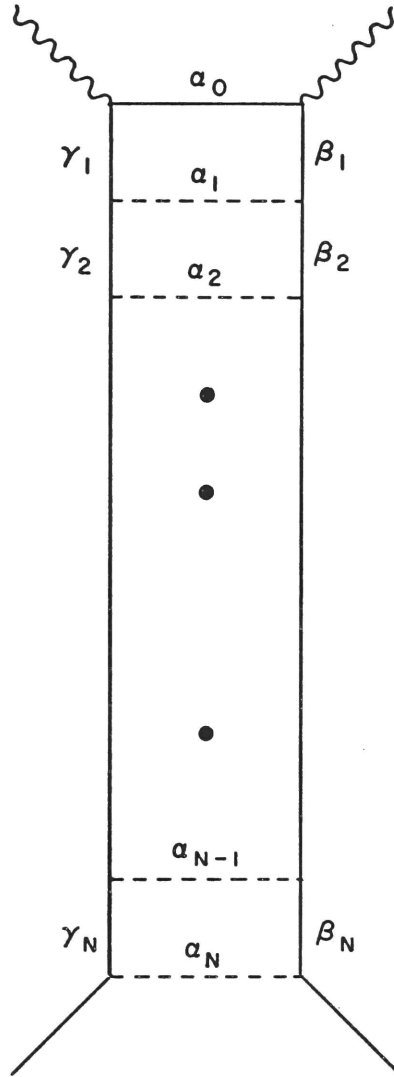


Fig. (II.2). Feynman Parameter Labelling of Ladder Diagrams

results in  $\mathcal{N}_{N\mu\nu}$  being formally independent of loop momenta and dependent only on Feynman parameters and external momenta. In each case we consider we will explicitly do this. For the

moment we assume  $\mathcal{N}_{N\mu\nu}$  is independent of loop momenta and proceed to perform the loop momenta integrations.

In order to perform the loop integrations we must diagonalize  $\psi$ . Following Eden et al <sup>13</sup> closely we linearly transform the loop momenta

$$k_j = \sum_{r=1}^N R_{jr} k'_r + S_j$$

so that  $\psi$  becomes

$$\psi = \sum_{j=1}^N c_j k_j'^2 + \frac{D}{C} \quad (\text{II.5})$$

where the matrix of  $R_{jr}$  is orthogonal; and  $c_j$ ,  $R_{jr}$ ,  $S_j$ ,  $D$  and  $C$  are functions only of external momenta and Feynman parameters. Since the Jacobian of this transformation is unity eq. (II.3) is transformed to

$$iT_{N\mu\nu} = \int d\Omega \mathcal{N}_{N\mu\nu} \prod_{j=1}^N \left[ \frac{d^4 k'_j}{(2\pi)^4} \right] \exp \left( i \prod_{r=1}^N c_r k_r'^2 + \frac{iD}{C} \right) \quad (\text{II.6})$$

Repeated use of the identity

$$\int_{-\infty}^{\infty} \frac{dx}{2\pi} e^{ix^2(A+i\epsilon)} = \frac{e^{i\pi/4}}{2\sqrt{\pi A}}$$

leads to

$$iT_{N\mu\nu} = \left( \frac{1}{16\pi^2 i} \right)^N \int d\Omega \mathcal{N}_{N\mu\nu} \frac{\exp\left(\frac{iD}{C}\right)}{C^2} \quad (\text{II.7})$$

with  $C = \prod_{j=1}^N c_j$  given in eq. (B4) and  $D$  given in eq. (B13) since their explicit expressions are cumbersome. Eq. (II.7) is the

general form of the (N+1) rung ladder diagram's contribution to the forward virtual Compton amplitude.

## B. The "Scalar Photon, Nucleon and Meson" Model

Abarbanel et al.<sup>9</sup> were the first to study a ladder model of the forward virtual Compton amplitude in the limit  $|q^2| \rightarrow \infty$  with  $\omega$  fixed. In their model all particles were assumed to be spinless. They wished to show in field theory that it was possible for the residue (which is a function of  $q^2$  but not  $\nu$ ) of the leading Regge trajectory to behave in such a way that scaling resulted in the structure function,  $W$ . They found  $\nu W$  scaled.

In order to illustrate our procedure and for the sake of completeness we will calculate the nucleon structure function in their model. There will be only one structure function due to the spinlessness of the photon.

The interaction Lagrangian density is given by

$$\mathcal{L}_{int} = e \psi^\dagger \psi W^0 + g \phi \psi^\dagger \psi \quad (\text{II.8})$$

where  $\psi$  is the nucleon field,  $W^0$  the photon field and  $\phi$  a scalar meson field. The scalar meson will be exchanged on the dashed line rungs of the ladder diagram of Fig. (II.1). We will begin our evaluation of the leading behavior of this ladder diagram with the expression

$$T_N = i \left( \frac{ig^2}{16\pi^2} \right)^N \int \frac{d\Omega}{c^2} e^{iD/C}$$



which follows from eq. (II.7) if we associate a factor of  $-ig$  with each meson-nucleon vertex and  $-i$  with each photon-nucleon vertex, as our interaction Lagrangian and normalization imply.

We will find the leading logarithmic behavior in  $|q^2|$  of  $T_N$  in the limit  $|q^2| \rightarrow \infty$  with  $\omega$  fixed by means of the Mellin transform technique.<sup>14</sup> The Mellin transform of a function,  $f$ , is defined to be

$$\tilde{f}(\eta) = \int_0^\infty f(t) t^{-\eta-1} dt \quad (\text{II.9})$$

and the inverse transform relation is

$$f(t) = \frac{1}{2\pi i} \int_C \tilde{f}(\eta) t^\eta d\eta \quad (\text{II.10})$$

where the contour  $C$  is parallel to the imaginary  $\eta$ -axis and  $\tilde{f}$  is analytic on  $C$ . A particularly important case is

$$f(t) = \frac{t^p (\ln t)^r}{r!} \quad (\text{II.11})$$

whose transform is

$$\tilde{f}(\eta) = \frac{1}{(\eta-p)^{r+1}} \quad (\text{II.12})$$

Since we wish to find the leading logarithm in  $|q^2|$  of  $T_N$  we will Mellin transform  $T_N$  in  $t = |q^2|$ , find the pole farthest to the right in the  $\eta$ -plane (called the leading pole), and use the correspondence given by eqns. (II.11) and (II.12) to find the leading logarithm of  $T_N$ . The coefficient of the leading logarithm is the residue of the transform of  $T_N$  evaluated at the leading pole.

All the momentum dependence of  $T_N$  is contained in

$$D = \alpha_0 q^2 (\rho d_{1N} + C') + JC$$

where  $\rho = 2q.p/q^2$  ; and  $d_{1N}$ ,  $C'$ ,  $C$  and  $J$  are independent of  $q^2$  and  $\rho$  . (They are defined in Appendix B.) As a result the Mellin transform <sup>15</sup> in  $|q^2|$  of  $T_N$  is  $(K_N = (ig^2/16\pi^2)^N)$

$$\tilde{T}_N(\eta) = K_N i^{\eta+1} \Gamma(-\eta) \int \frac{d\Omega e^{iJ}}{C^{2+\eta}} \alpha_0^\eta (\rho d_{1N} + C')^\eta \quad (\text{II.13})$$

with  $\text{Re}\eta < 0$ . The leading pole is at  $\eta = -1$ . It can be made explicit by partially integrating with respect to  $\alpha_0$

$$\tilde{T}_N = \frac{-K_N i^{\eta+1} \Gamma(-\eta)}{\eta + 1} \int d\Omega \alpha_0^{\eta+1} \frac{d}{d\alpha_0} \left[ \frac{e^{iJ}}{C^{2+\eta}} (\rho d_{1N} + C')^\eta \right]$$

Since there are no other singularities at  $\eta = -1$  the leading logarithmic term of  $T_N$  is

$$\begin{aligned} T_N &\sim \frac{-K_N}{|q^2|} \int d\Omega \frac{d}{d\alpha_0} \left[ \frac{e^{iJ}}{C(\rho d_{1N} + C')} \right] \\ &\sim \frac{K_N}{|q^2|} \int \frac{d\Omega'}{C'} \frac{e^{iJ'}}{\rho d_{1N} + C'} \end{aligned} \quad (\text{II.14})$$

where we have performed the  $\alpha_0$  integration in the last line (which is equivalent to setting  $\alpha_0 = 0$  since the upper bound of the  $\alpha_0$  integration does not give a contribution). The primes on  $C'$  and  $J'$  indicate  $\alpha_0$  is equal to zero in them, and  $d\Omega' = d\alpha_1 d\alpha_2 \dots d\alpha_N d\beta_1 \dots d\beta_N d\gamma_1 \dots d\gamma_N$ . Eq. (II.14) gives the leading behavior in  $|q^2|$  of  $T_N$  in the limit  $|q^2| \rightarrow \infty$  with  $\omega = |\rho|$  fixed.

If we now assume that  $\omega$  is very large then we may approximate the integral in eq. (II.14) with its leading logarithmic behavior in  $\omega$ . This region of the variables is where Regge behavior is expected to occur.

The Mellin transform in  $\rho$  of  $T_N$  as given by eq. (II.14) is

$$\tilde{T}_N \sim \frac{K_N}{|q^2|} [-\pi \csc(\pi\eta)] \int \frac{d\Omega'}{C^{2+\eta}} e^{iJ'} d_{1N}^\eta \quad \text{Re}\eta < 0 \quad (\text{II.15})$$

There is a multiple pole at  $\eta = -1$  coming from the  $\csc\eta$  factor and the integrations over  $\alpha_1, \alpha_2, \dots, \alpha_N$ . Partially integrating with respect to  $\alpha_1, \alpha_2, \dots, \alpha_N$  gives

$$\tilde{T}_N \sim \frac{K_N}{|q^2|} \frac{(-\pi \csc\pi\eta)}{(\eta+1)^N} (-1)^N \int d\Omega' d_{1N}^{\eta+1} \frac{d^N}{d\alpha_1 d\alpha_2 \dots d\alpha_N} \left[ \frac{e^{iJ'}}{C^{2+\eta}} \right] \quad (\text{II.16})$$

Corresponding to the pole of order  $N+1$  at  $\eta = -1$  is the following leading logarithmic behavior in  $\rho$

$$T_N \sim \frac{K_N}{|q^2| \rho} \frac{(1 \ln \rho)^N}{N!} \int_0^\infty \frac{d\beta_1 d\beta_2 \dots d\beta_N d\gamma_1 d\gamma_2 \dots d\gamma_N}{C''} e^{iJ''} \quad (\text{II.17})$$

$$\sim \frac{K_N}{|q^2| \rho} \frac{(1 \ln \rho)^N}{N!} \left[ \int_0^\infty \frac{d\beta d\gamma}{\beta + \gamma} e^{-i(\beta + \gamma)(M^2 - ie)} \right]^N \quad (\text{II.18})$$

$$\sim \frac{1}{|q^2| \rho} \frac{1}{N!} \left( \frac{g^2 1 \ln \rho}{16\pi^2 M^2} \right)^N. \quad (\text{II.19})$$

After evaluating the residue at  $\eta = -1$  in eq. (II.16) we performed the  $\alpha_1, \alpha_2, \dots, \alpha_N$  integrations and obtained eq. (II.17) where the double primes signify all  $\alpha_i = 0$  in the primed quantities. From eq. (B17) it is clear that  $C'' = \prod_{j=1}^N (\beta_j + \gamma_j)$ . This together with the expression for  $J''$  implied by eq. (B13) leads to eq. (II.18).

After evaluating the simple integral in eq. (II.18) we obtain eq. (II.19). To find the contribution of this ladder diagram to the inelastic structure we take the imaginary part of  $T_N$  as indicated in eq. (I.16)

$$W_N = \frac{g^2}{16\pi^2 M^2 |q^2| \omega(N-1)!} \left( \frac{g^2 \ln \omega}{16\pi^2 M^2} \right)^{N-1}$$

where we use  $\omega = |\rho|$ . Upon summing  $W_N$  from  $N=1$  to  $\infty$  we obtain eq. (I.17), which is the result of Abarbanel et al. Therefore,  $q.pW$  scales.

### C. The Vector Photon, "Scalar Nucleon" and Scalar Meson Model

Altarelli and Rubinstein<sup>10</sup> studied a ladder model for the virtual Compton amplitude which differed from the model of Abarbanel et al. only in the spin it assigned to the photon. Altarelli and Rubinstein took the spin of the photon to be one and consequently used the following interaction Lagrangian:

$$\mathcal{L}_{\text{int}} = -ie\psi^* \partial_\mu \psi A^\mu + g\psi^* \psi \phi \quad (\text{II.20})$$

where  $A^\mu$  is the electromagnetic field,  $\phi$  is the scalar meson field and  $\psi$  is the nucleon field with  $\psi^*$  its Hermitian conjugate. Scaling was found in  $\nu W_2$  but  $W_1$  failed to scale by a factor of  $|q^2|^{-1} \ln|q^2|$  (except trivially at  $|q^2| \rightarrow \infty$ ).

The calculation of the virtual Compton amplitude differs from that of Abarbanel et al. because loop momenta now appear in  $\mathcal{N}_{N\mu\nu}$ . The nucleon-photon vertex contributes a factor of  $-i(p+p')_\mu$  to  $\mathcal{N}_{N\mu\nu}$  where  $p$  is the incoming and  $p'$  the out-

going nucleon momentum at the vertex. As a result

$$\mathcal{N}_{N\mu\nu} = (-1)^{N+1} g^{2N} (2k_1+q)_\mu (2k_1+q)_\nu. \quad (\text{II.21})$$

From eq. (I.14) it is clear that the contribution to  $T_1$  from  $T_{N\mu\nu}$  will be the coefficient of  $-g_{\mu\nu}$  and the contribution to  $T_2$  will be the coefficient of  $p_\mu p_\nu / M^2$ . Therefore we may use

$$\mathcal{N}'_{N\mu\nu} = (-1)^{N+1} g^{2N} 4k_{1\mu} (q+k_1)_\nu \quad (\text{II.22})$$

instead of  $\mathcal{N}_{N\mu\nu}$  in evaluating  $T_{N\mu\nu}$  since the coefficients of  $g_{\mu\nu}$  and  $p_\mu p_\nu$  are the same in both cases (and these are all we need to obtain  $T_1$  and  $T_2$ ). The  $q_\mu$  or  $q_\nu$  dependent terms are irrelevant to our purposes.

We now introduce two "dummy" momenta which will allow us to rewrite  $\mathcal{N}'_{N\mu\nu}$  as a derivative expression in these momenta and make it independent of the loop momentum  $k_1$ . Afterwards the "dummy" momenta  $A_0$  and  $A_1$  will be set equal to zero. The momenta are introduced as in Fig. II.3. As a result  $\psi$  is modified in eq. (II.4) so that

$$\alpha_0 [(q+k_1)^2 - M^2] + (\beta_1 + \gamma_1) (k_1^2 - M^2)$$

is replaced with

$$\alpha_0 [(q+k_1+A_0)^2 - M^2] + (\beta_1 + \gamma_1) [(k_1+A_1)^2 - M^2]$$

in  $\psi$ . Consequently, we may rewrite  $k_{1\mu}$  as  $[2i(\beta_1 + \gamma_1)]^{-1} \frac{\partial}{\partial A_1^\mu}$  and  $(q+k_1)_\nu$  as  $[2i\alpha_0]^{-1} \frac{\partial}{\partial A_0^\nu}$  in  $\mathcal{N}'_{N\mu\nu}$ . Therefore

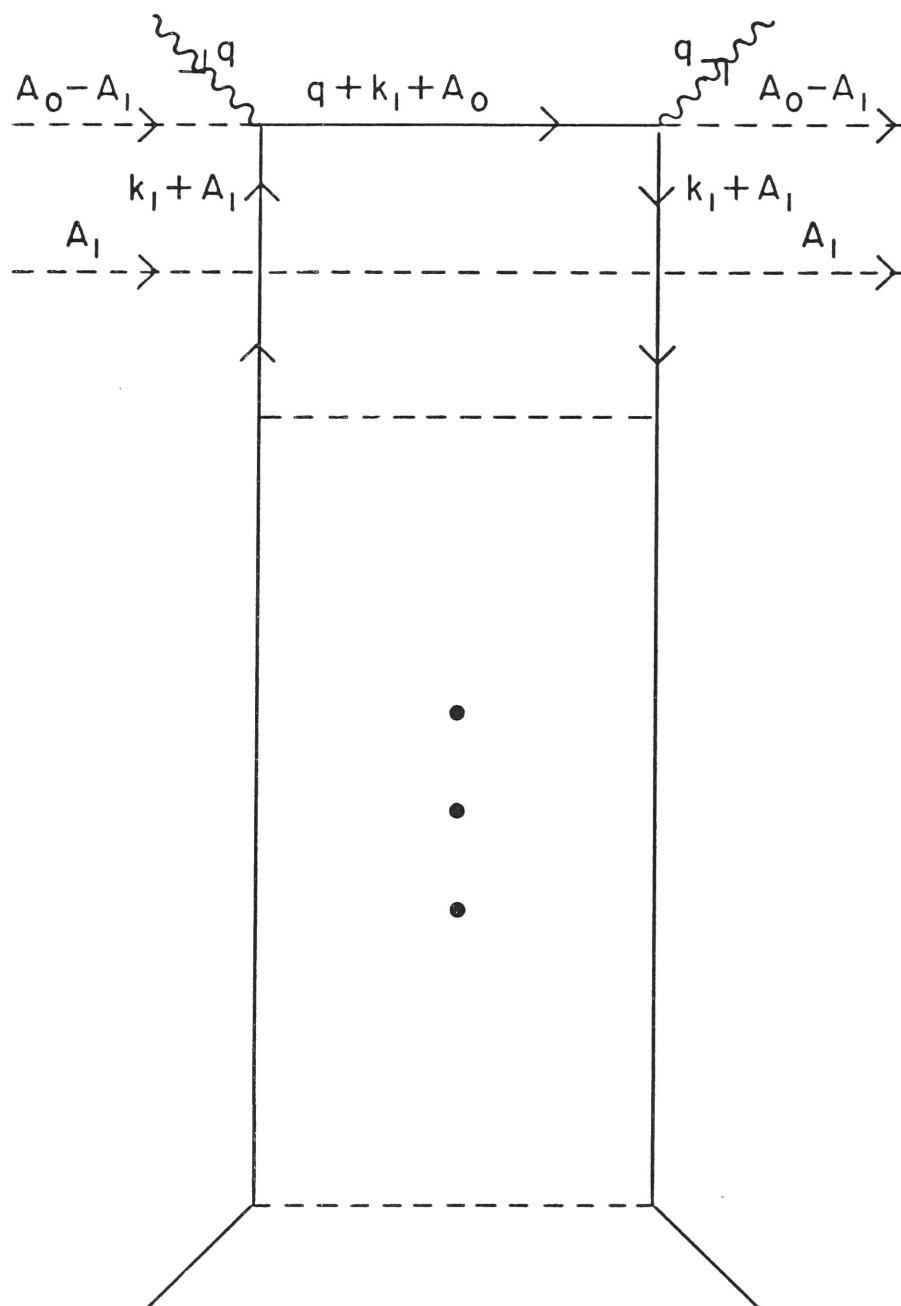


Fig. II.3. Ladder Diagram With "Dummy" Momenta

$$iT_{N\mu\nu} \equiv (-1)^{N+1} \left( \frac{g^2}{16\pi^2 i} \right)^N \int \frac{d\Omega'}{(2i)^2 \alpha_0 (\beta_1 + \gamma_1)} \frac{\partial}{\partial A_0^\nu} \frac{\partial}{\partial A_1^\mu} \left[ \frac{e^{iD/C}}{C^2} \right]_{A_0=A_1=0}$$

where  $D$  is now a function of  $A_0$  and  $A_1$  and  $C$  is unchanged.

The function  $D$  is given by eq. (B6) if we set  $A_2 = A_3 = \dots = A_N = 0$  in the right side of that equation. In Appendix C we show how to evaluate derivatives of  $\exp\left(\frac{iD}{C}\right)$ . Consequently

$$T_{N\mu\nu} \equiv 4i \left( \frac{ig^2}{16\pi^2} \right)^N \int \frac{d\Omega}{C^2} \left\{ \frac{(0)_\nu (i)_\mu}{C^2} + \frac{g_{\mu\nu} (01)}{2iC} \right\} \exp\left(\frac{iD}{C}\right)$$

in the notation defined in Appendix C. If we drop terms proportional to  $q_\mu$  or  $q_\nu$  then  $T_{N\mu\nu}$  becomes

$$T_{N\mu\nu} \equiv 4i K_N \int \frac{d\Omega}{C^2} \left\{ \frac{d_{1N}^2 p_\mu p_\nu}{C^2} - \frac{C_N^1}{2iC} g_{\mu\nu} \right\} e^{iD/C} \quad (\text{II.23})$$

using eqns. (C1), (C2), and (C5). Comparing eq. (II.23) with eq. (I.14) implies

$$T_{1N} = 2K_N \int \frac{d\Omega}{C^3} C_N^1 \exp\left(\frac{iD}{C}\right) \quad (\text{II.24})$$

$$T_{2N} = 4M^2 i K_N \int \frac{d\Omega}{C^4} d_{1N}^2 \exp\left(\frac{iD}{C}\right) \quad (\text{II.25})$$

The evaluation of the leading logarithmic behavior of  $T_{2N}$  is precisely the same as that of  $T_N$  in the previous section up to eq. (II.15) where the additional factor of  $d_{1N}$  in the numerator of  $T_{2N}$  suppresses the leading pole two units to the left at  $\eta = -3$ . As a result we may read the leading behavior of  $T_{2N}$  from eq. (II.19) if we take account

of the new position of the leading pole of the Mellin transform in  $\rho$  :

$$T_{2N} \sim \frac{4M^2}{|q^2| \rho^3 N!} \left( \frac{g^2 \ln \rho}{16\pi^2 M^2} \right)^N \quad (\text{II.26})$$

The contribution of the (N+1) rung ladder diagram to the inelastic structure function  $W_2$  is

$$W_{2N} \sim \frac{g^2}{4\pi^2 |q^2| \omega^3} \frac{1}{(N-1)!} \left( \frac{g^2 \ln \omega}{16\pi^2 M^2} \right)^{N-1} \quad (\text{II.27})$$

which gives eq. (I.18a) upon summation over N.

The evaluation of the leading logarithmic behavior of  $T_{1N}$  differs from the previous cases. The difference appears when we find the leading pole of the Mellin transform<sup>15</sup> in  $|q^2|$  of  $T_{1N}$ :

$$\tilde{T}_{1N} = 2 K_N i^\eta \Gamma(-\eta) \int \frac{d\Omega}{C^{3+\eta}} C_N^1 e^{iJ} \alpha_0^\eta (\rho d_{1N} + C')^\eta \quad \text{Re} \eta < 0$$

The leading pole is at  $\eta = -1$  but it is of order two as opposed to order one in the previous cases. Besides a pole factor from the  $\alpha_0$  integration there will be another pole factor which can be manifested if we "scale" the variables  $\alpha_0, \alpha_1, \beta_1$  and  $\gamma_1$ . This "scaling" has nothing to do with our use of the term in relation to the inelastic structure functions previously. Scaling the above Feynman parameters means to perform the following transformation of variables:



$$\begin{aligned}
\alpha_0 &= x \tilde{\alpha}_0 \\
\alpha_1 &= x \tilde{\alpha}_1 \\
\beta_1 &= x \tilde{\beta}_1 \\
\gamma_1 &= x \tilde{\gamma}_1 = x (1 - \tilde{\alpha}_0 - \tilde{\alpha}_1 - \tilde{\beta}_1)
\end{aligned} \tag{II.28}$$

which has the Jacobian  $x^3$ . The polynomial,  $C$ , becomes

$$C = x\tilde{C}$$

due to its homogeneous nature where  $\tilde{C}$  is such that  $\tilde{C}/x$  is not a polynomial in  $x$ . Therefore

$$\begin{aligned}
\tilde{T}_{1N} &= 2K_N i^\eta \Gamma(-\eta) \int_0^1 d\tilde{\alpha}_0 d\tilde{\alpha}_1 d\tilde{\beta}_1 d\tilde{\gamma}_1 \int_0^\infty \frac{dx d\alpha_2 \dots d\alpha_N d\beta_2 \dots d\beta_N d\gamma_2 \dots d\gamma_N}{\tilde{C}^{3+\eta}} \\
&\cdot \tilde{C}_N^1 e^{iJ} (\tilde{\alpha}_0 x)^\eta (\rho d_{1N} + \tilde{C}')^\eta \delta(1 - \tilde{\alpha}_0 - \tilde{\alpha}_1 - \tilde{\beta}_1 - \tilde{\gamma}_1)
\end{aligned}$$

Partially integrating with respect to  $\alpha_0$  and  $x$  leads to a double pole at  $\eta = -1$ . This implies

$$\begin{aligned}
T_{1N} &\sim \frac{2 K_N \ln|q^2|}{i|q^2|} \int_0^1 d\tilde{\alpha}_1 d\tilde{\beta}_1 d\tilde{\gamma}_1 \int_0^\infty d\alpha_2 \dots d\alpha_N d\beta_2 \dots d\beta_N d\gamma_2 \dots d\gamma_N \\
&\cdot \frac{\tilde{C}_N^{1'} e^{iJ'} \delta(1 - \tilde{\alpha}_1 - \tilde{\beta}_1 - \tilde{\gamma}_1)}{\tilde{C}^2(\rho d_{1N} + \tilde{C}')} \bigg|_{\tilde{\alpha}_0 = x = 0} \tag{II.29}
\end{aligned}$$

Due to setting  $\tilde{\alpha}_0 = x = 0$  we have  $J'$  independent of  $\tilde{\alpha}_0$ ,  $\tilde{\alpha}_1$ ,  $\tilde{\beta}_1$  and  $\tilde{\gamma}_1$ ; and from eq. (B17) and the delta function  $\tilde{C} = \tilde{C}' = \tilde{C}_N^{1'}$  where  $\tilde{C}_N^{1'}$  is  $\tilde{C}_N^1$  with  $\alpha_1 = 0$ .

The evaluation of the leading  $\rho$  behavior of  $T_{1N}$  proceeds exactly as in the case of  $T_N$  in the last section except that we lose one factor of the integral in eq. (II.18) due to our scaling of the Feynman parameters of the first loop. Therefore

$$T_{1N} \sim \frac{2 K_N \ln |q^2|}{i |q^2| \rho} \frac{(1n\rho)^N}{N!} \left[ \int_0^\infty \frac{d\beta d\gamma}{\beta + \gamma} e^{-i(\beta + \gamma)M^2} \right]^{N-1} \quad (II.30)$$

$$\sim \frac{2M^2 \ln |q^2|}{|q^2| \rho N!} \left( \frac{g^2 1n\rho}{16\pi^2 M^2} \right)^N$$

and

$$W_{1N} \sim \frac{g^2 1n |q^2|}{8\pi^2 |q^2| \omega} \frac{1}{(N-1)!} \left( \frac{g^2 1n\omega}{16\pi^2 M^2} \right)^{N-1} \quad (II.31)$$

which gives eq. (I.18b) upon summation over  $N$ .

## CHAPTER III

Spin  $\frac{1}{2}$  Nucleon Models

## A. Introduction

In chapter II we described previously studied models of the virtual Compton amplitude in which the nucleon was treated as a spinless particle. In reality the nucleons have spin  $\frac{1}{2}$ . It is possible that spin is an inessential complication in this type of model, and that models taking the actual spin of the nucleons into account would not modify the qualitative features of the inelastic structure function calculations. In particular, the hope was that the scaling of  $\nu W_2$  in eq. (I.18a) would not depend on the spinlessness of the nucleons in that model.

Unfortunately a calculation of the contribution to  $\nu W_2$  of the diagram in Fig. (III.1) with the solid lines being spin  $\frac{1}{2}$  nucleons and the dashed line a neutral vector meson resulted in a term behaving as  $\ln|q^2|$  times a function that scaled.<sup>17</sup> Thus it appeared that deviations from scaling could occur in models with a presumably more realistic (since the nucleon's physical spin was taken into account) nucleon behavior.

In order to further investigate the non-scaling behavior of this neutral vector meson theory with spin  $\frac{1}{2}$  nucleons we considered a model for the virtual Compton amplitude consisting of a sum of ladder diagrams (Fig. II.1) with spin  $\frac{1}{2}$  nucleons and neutral vector mesons exchanged on the rungs of the ladder. Section III.B describes this calculation. It became apparent that this calculation was essentially the same as the corresponding calculation in a  $\gamma_5$  pseudoscalar meson model in which pseudo-

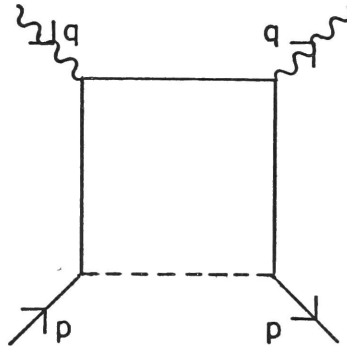


Fig. III.1. A Compton Amplitude Diagram

scalar mesons were exchanged on the rungs of the ladders. Section III.C develops the results of this model.

The Feynman parameter integrals giving the leading logarithmic behavior of the models of sections III.B and III.C are closely related to those of a truss bridge diagram model studied by Bjorken and Wu.<sup>18</sup> Consequently we study a truss bridge diagram model in section III.D.

The structure functions in this model are intermediate between those calculated in chapter II and those of the spin  $\frac{1}{2}$  nucleon models of chapter III.

#### B. The Neutral Vector Meson Model

The interaction Lagrangian in the neutral vector meson model is

$$- : e \bar{\psi} \gamma_{\mu} \psi A^{\mu} : - : g \bar{\psi} \gamma_{\mu} \psi B^{\mu} :$$

with  $\psi$  the nucleon field,  $A_{\mu}$  the electromagnetic field,  $B^{\mu}$  the neutral vector meson field and  $g$  the meson-nucleon coupling constant. We use the vector meson propagator in the Feynman gauge, i.e.

$$\frac{-ig_{\mu\nu}}{k^2 - m^2}$$

where  $k$  is the meson four-momentum and  $m$  its mass. The contribution of the  $N+1$  rung ladder diagram (Fig. (II.1)) to the virtual Compton amplitude is given by eq. (II.1) with

$$\begin{aligned} \mathcal{N}_{N\mu\nu} &= \frac{-g^{2N}}{4M} \text{Tr}[\gamma_{\mu}(q+k_1+M)\gamma_{\nu}P_N] \\ &= \frac{-g^{2N}}{4M} P_N \end{aligned}$$

and  $P_N$  defined in eq. (A1). The trace expression results from spin averaging the nucleon.

In Appendix A we show that  $P_N$  may be written

$$P_N = p_N^a + p_N^b \not{x} + \sum_{j=1}^N p_N^j \not{x}_j$$

where  $p_N^a$ ,  $p_N^b$  and  $p_N^j$  are scalar functions of momenta for  $j=1,2,\dots,N$ . Consequently,

$$\begin{aligned} -\frac{1}{4} \mathcal{P}_N &= g_{\mu\nu} [MP_N^a - (q+k_1) \cdot (p_N^b + \sum_{j=1}^N k_j \tilde{p}_N^j)] + (q+k_1)_{\mu} (p_{\nu} p_N^b + \\ &+ \sum_{j=1}^N \tilde{p}_N^j k_{j\nu}) + (q+k_1)_{\nu} (p_{\mu} p_N^b + \sum_{j=1}^N \tilde{p}_N^j k_{j\mu}) \end{aligned}$$

Due to the appearance of  $k_1, k_2, \dots, k_N$  in  $P_N$  we introduce "dummy" external momenta,  $A_0, A_1, \dots, A_N$  into  $\psi$  ( in the same manner that we did in section II.C) as indicated in Fig. (III.2):

$$\psi = \alpha_0 [(q+k_1+A_0)^2 - M^2] + \sum_{r=1}^N \{ (\beta_r + \gamma_r) [(k_r + A_r)^2 - M^2] + \alpha_r [(k_{r+1} - k_r)^2 - m^2] \}$$

Therefore if a term in  $P_N$  were linear in  $k_j$  we would replace  $k_{j\lambda}$  with

$$\frac{1}{2i(\beta_j + \gamma_j)} \frac{\partial}{\partial A_j^\lambda} \quad (III.1a)$$

and if the term were quadratic in  $k_j$  we replace  $k_{j\lambda} k_{j\sigma}$  with

$$\frac{1}{(2i)^2 (\beta_j + \gamma_j)^2} \left[ \frac{\partial^2}{\partial A_j^\lambda \partial A_j^\sigma} - 2i(\beta_j + \gamma_j) g_{\lambda\sigma} \right] \quad (III.1b)$$

Thus  $P_N$  can be made independent of loop momenta and we can perform loop integrations. After performing the loop integrations we apply the derivative operators and then set all dummy momenta equal to zero.

The first part of  $P_N$  we will evaluate is  $(q+k_1)_\mu p_\nu p_N^b$ . In Appendix A we show

$$P_N^b = 2^N \prod_{j=1}^N (k_j^2 - M^2)$$

and because of its simple form we need not use the dummy momenta  $A_1, A_2, \dots, A_N$  (setting them equal to zero immediately). Instead we replace  $P_N^b$  by

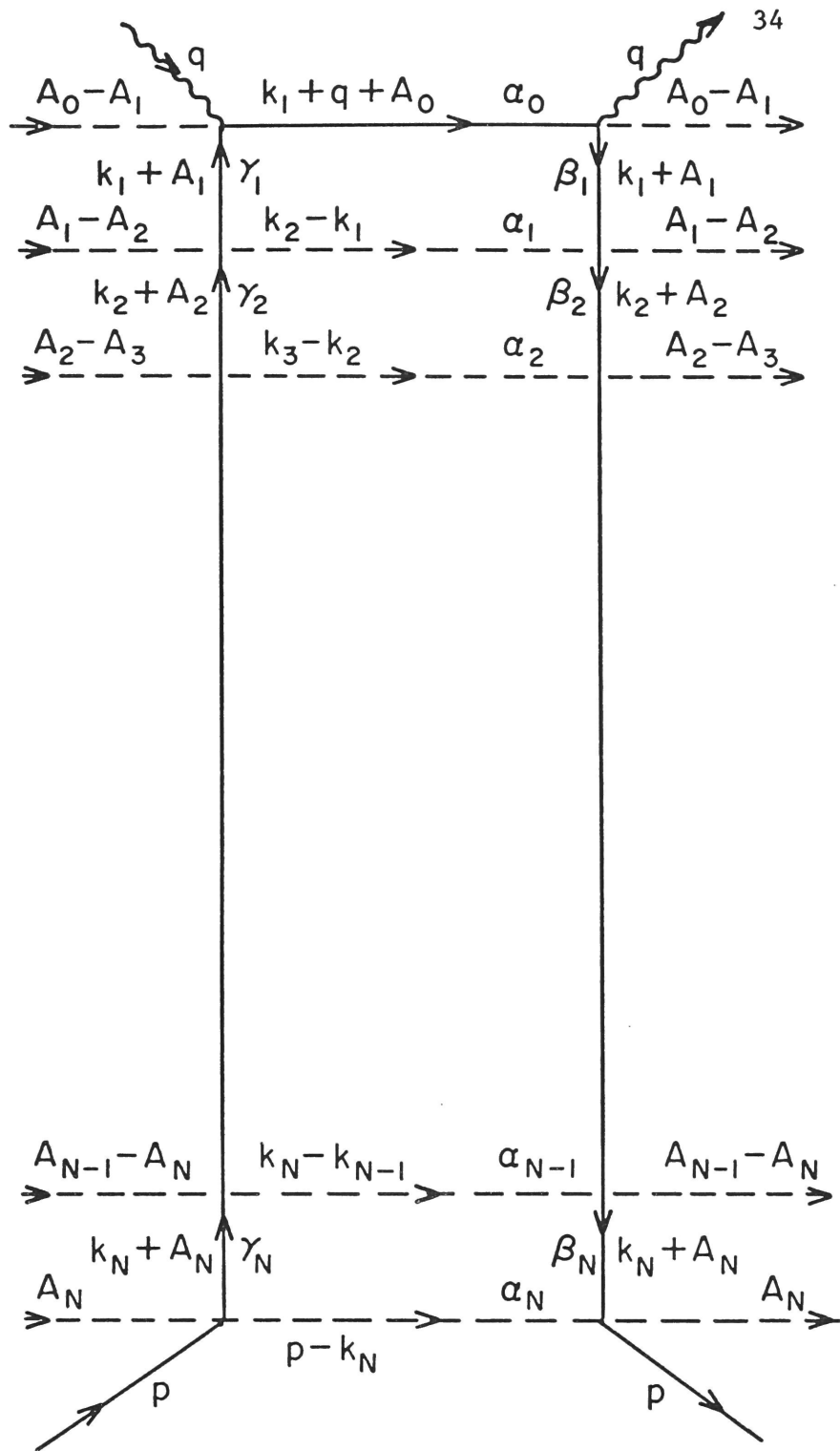


Fig. III.2. Ladder Diagram With All "Dummy" Momenta Introduced

$$\frac{2^N}{i^N} \prod_{j=1}^N \frac{\partial}{\partial \gamma_j}$$

which reproduces  $P_N^b$  if applied to  $\exp(i\psi)$ . In addition  $(q+k_1)_\mu$  is replaced by  $(2i\alpha_0)^{-1} \partial/\partial A_0^\mu$ . Therefore the contribution to  $T_{N\mu\nu}$  of this term is

$$\mathcal{L}_{N\mu\nu} = \frac{ip_\nu}{M} \left( \frac{-g^2}{8\pi^2} \right)^N \int_0^\infty \frac{d\Omega}{2i\alpha_0} \frac{\partial}{\partial A_0^\mu} \prod_{j=1}^N \frac{\partial}{\partial \gamma_j} \frac{\exp(\frac{iD}{C})}{C^2} \Big|_{A_0=0}$$

The integrations with respect to  $\gamma_1, \gamma_2, \dots, \gamma_N$  can be performed and only the lower bounds  $\gamma_1 = \gamma_2 = \dots = \gamma_N = 0$  contribute. After performing the dummy momentum derivative we obtain

$$\mathcal{L}_{N\mu\nu} = \frac{ip_\nu}{M} \left( \frac{g^2}{8\pi^2} \right)^N \int_0^\infty \frac{d\Omega}{C^3} (p_\mu d_{1N} + q_\mu C') \exp\left(\frac{iD}{C}\right)$$

where it is understood that all  $\gamma_j$  are set equal to zero in the expressions for  $D$  and  $C$  which are given in eqns. (B4) and (B13):

$$D = D(0) = \alpha_0 q^2 (\rho d_{1N} + C') + JC$$

with  $C' = C|_{\alpha_0=0}$ ,  $d_{ij} = \alpha_i \alpha_{i+1} \dots \alpha_j$ , and  $\rho = 2q \cdot p / q^2 (\omega = |\rho|)$ . We keep the  $p_\mu p_\nu$  part of  $\mathcal{L}_{N\mu\nu}$  since it will eventually lead to a contribution to  $T_2$ :

$$\mathcal{L}_N = \frac{i}{M} \left( \frac{g^2}{8\pi^2} \right)^N \int_0^\infty \frac{d\Omega}{C^3} d_{1N} \exp\left(\frac{iD}{C}\right). \quad (\text{III.2})$$

The use of the Mellin transform technique will enable us to find the leading asymptotic behavior of  $\mathcal{L}_N$ . We first determine the leading  $|q^2|$  behavior of  $\mathcal{L}_N$  for fixed  $\rho$ .

The Mellin transform of  $\mathcal{L}_N$  in  $w = |q^2|$  is <sup>15</sup>



$$\begin{aligned}\tilde{\mathcal{L}}_N &= \int_0^\infty dw w^{-\eta-1} \mathcal{L}_N \\ &= \frac{i}{M} \left(\frac{g^2}{8\pi^2}\right)^N i^\eta \Gamma(-\eta) \int_0^\infty \frac{d\Omega}{C^{3+\eta}} d_{1N}^{\alpha_0 \eta} (\rho d_{1N} + C')^\eta e^{iJ}. \quad \text{Re} \eta < 0\end{aligned}$$

$\tilde{\mathcal{L}}_N$  is defined for  $\text{Re} \eta > -1$  but becomes divergent at  $\eta = -1$  since the  $\alpha_0$  integration then diverges. There are additional divergences in  $\tilde{\mathcal{L}}_N$  at  $\eta = -1$  which can be brought out by scaling over various sets of Feynman parameters. Let

$$\begin{aligned}\alpha_0 &= x_1 x_2 x_3 \dots x_N \tilde{\alpha}_0 \\ \alpha_1 &= x_1 x_2 \dots x_N \tilde{\alpha}_1 \\ \beta_1 &= x_1 \dots x_N \tilde{\beta}_1 = x_1 \dots x_N (1 - \tilde{\alpha}_0 - \tilde{\alpha}_1) \\ \alpha_2 &= x_2 x_3 \dots x_N \tilde{\alpha}_2 \\ \beta_2 &= x_2 x_3 \dots x_N \tilde{\beta}_2 = x_2 x_3 \dots x_N [1 - x_1 (\tilde{\alpha}_0 + \tilde{\alpha}_1 + \tilde{\beta}_1) - \tilde{\alpha}_2] \\ \alpha_3 &= x_3 x_4 \dots x_N \tilde{\alpha}_3 \\ &\vdots \\ \alpha_N &= x_N \tilde{\alpha}_N\end{aligned}\tag{III.3}$$

$$\begin{aligned}\beta_N &= x_N \tilde{\beta}_N = x_N [1 - x_1 x_2 \dots x_{N-1} (\tilde{\alpha}_0 + \tilde{\alpha}_1 + \tilde{\beta}_1) - x_2 x_3 \dots x_{N-1} (\tilde{\alpha}_2 + \tilde{\beta}_2) - \\ &\quad - \dots - x_{N-1} (\tilde{\alpha}_{N-1} + \tilde{\beta}_{N-1}) - \tilde{\alpha}_N]\end{aligned}$$

The Jacobian for this transformation is  $x_1^2 x_2^4 x_3^6 \dots x_N^{2N}$  and the homogeneous polynomial,  $C$ , becomes  $x_1^2 x_2^3 \dots x_N^N \tilde{C}$  where  $\tilde{C}$  is a polynomial in  $x_1, x_2, \dots, x_N$  and  $\tilde{C}/x_i$  is not a polynomial for  $i=1, 2, \dots, N$ .

Under this transformation  $\tilde{\mathcal{L}}_N$  becomes

$$\tilde{\mathcal{L}}_N = \frac{i}{M} \left( \frac{g^2}{8\pi^2} \right)^N i^{\eta} \Gamma(-\eta) \int_0^1 d\tilde{\Omega} \int_0^\infty \frac{dx_1 dx_2 \dots dx_N}{\tilde{C}^{3+\eta}} \cdot \tilde{d}_{1N} (\alpha_0 x_1 x_2 \dots x_N)^\eta (\rho d_{1N} + \tilde{C}')^\eta e^{iJ} (1 - \tilde{\alpha}_0 - \tilde{\alpha}_1 - \tilde{\beta}_1) \cdot \delta(1 - x_1 (\tilde{\alpha}_0 + \tilde{\alpha}_1 + \tilde{\beta}_1) - \tilde{\alpha}_2) \dots$$

where  $d\tilde{\Omega}$ ,  $\tilde{d}_{1N}$ , and  $\tilde{C}$  have  $\alpha_i$  and  $\beta_i$  replaced with  $\tilde{\alpha}_i$  and  $\tilde{\beta}_i$ , and each term in  $J$  contains at least one factor of  $x_i$  for some  $i$ . The Dirac delta functions,  $\delta(x)$ , implement the constraints in the scaling (eq. (III.3)).

We can now partially integrate  $N+1$  times and exhibit the integral's singularity at  $\eta=-1$

$$\tilde{\mathcal{L}}_N = (-1)^{N+1} \frac{i}{M} \left( \frac{g^2}{8\pi^2} \right)^N i^{\eta} \Gamma(-\eta) \int_0^1 d\tilde{\Omega} \int_0^\infty dx \frac{(\tilde{\alpha}_0 x_1 x_2 \dots x_N)^{\eta+1}}{(\eta+1)^{N+1}} \frac{\partial^{N+1}}{\partial \tilde{\alpha}_0 \partial x_1 \partial x_2 \dots \partial x_N} \cdot \frac{d_{1N} (\rho d_{1N} + \tilde{C}')^\eta}{\tilde{C}^{3+\eta}} e^{iJ} \delta(1 - \tilde{\alpha}_0 - \tilde{\alpha}_1 - \tilde{\beta}_1) \delta(1 - x_1 (\tilde{\alpha}_0 + \tilde{\alpha}_1 + \tilde{\beta}_1) - \tilde{\alpha}_2) \dots$$

with  $dx = dx_1 dx_2 \dots dx_N$ .

Since the leading singularity is an  $(N+1)$  order pole at  $\eta=-1$  the leading asymptotic behavior of  $\mathcal{L}_N$  in  $|q^2|$  (for fixed  $\rho$ ) is given by  $|q^2|^{-1} (N!)^{-1} (\ln|q^2|)^N$  times the residue of  $\tilde{\mathcal{L}}_N$  at  $\eta=-1$ :

$$\mathcal{L}_N \rightarrow \frac{1}{M|q^2|N!} \left( \frac{g^2 \ln|q^2|}{8\pi^2} \right)^N \int_0^1 \frac{d\Omega' d_{1N}^{\delta(1-\alpha_1-\beta_1)\delta(1-\alpha_2-\beta_2)\dots\delta(1-\alpha_N-\beta_N)}}{C'^2(\rho d_{1N} + C')} \quad (III.4)$$

where we have dropped the tilde over the Feynman parameters and let  $d\Omega' = d\alpha_1 d\alpha_2 \dots d\alpha_N d\beta_1 d\beta_2 \dots d\beta_N$ . Eq. (III.4) displays the leading  $|q^2|$  behavior of  $\mathcal{L}_N$  for fixed  $\rho$ .

We now find the leading  $\rho$  behavior of the remaining Feynman parameter integral through the use of Mellin transforms. The Mellin transform of eq. (III.4) in  $w=\rho$  gives<sup>16</sup>

$$\frac{1}{M|q^2|N!} \left( \frac{g^2 \ln|q^2|}{8\pi^2} \right)^N (-\pi \csc \pi \eta) \int_0^1 \frac{d\Omega' d_{1N}^{1+\eta} \delta(1-\alpha_1-\beta_1)\dots\delta(1-\alpha_N-\beta_N)}{C'^{3+\eta}} \quad (III.5)$$

There is a pole of order 1 at  $\eta=-1$  due to the  $\csc \pi \eta$  factor; and a pole of order  $N+1$  at  $\eta=-2$  due to the  $\csc \pi \eta$  factor and the poles which appear upon partially integrating with respect to  $\alpha_1, \alpha_2, \dots, \alpha_N$  in the same manner as above. The result, after evaluating the residues at the various poles, is

$$\begin{aligned} \mathcal{L}_N \rightarrow & \frac{1}{M|q^2|\rho N!} \left( \frac{g^2 \ln|q^2|}{8\pi^2} \right)^N \int_0^1 \frac{d\Omega' \delta(1-\alpha_1-\beta_1)\delta(1-\alpha_2-\beta_2)\dots\delta(1-\alpha_N-\beta_N)}{C'^2} - \\ & - \frac{1}{M|q^2|\rho^2(N!)} \left( \frac{g^2 K_1 \ln|q^2| \ln \rho}{8\pi^2} \right)^N \end{aligned}$$

where

$$K_1 = \int_0^1 \frac{d\beta \delta(1-\beta)}{\beta} = 1 \quad (III.6)$$

The first term gives no contribution to the absorptive part of  $T_{\mu\nu}$  when summed over  $N$  so we drop it from consideration. Thus the contribution of the  $p_\mu(q+k_1)_\nu P_N^b + p_\nu(q+k_1)_\mu P_N^b$  term to the  $p_\mu p_\nu$  part of  $T_{N\mu\nu}$  is:

$$\frac{-2p_\mu p_\nu}{M|q^2|\rho^2(N!)} \left( \frac{g^2 K_1 \ln|q^2| \ln \rho}{8\pi^2} \right)^N \quad (\text{III.7})$$

The next term we examine is  $-g_{\mu\nu}(q+k_1) \cdot p P_N^b$ . The calculation of the leading contribution of this term to  $T_{N\mu\nu}$  is very similar to the calculation just completed. The Feynman parameter integral for this term is given by the right side of eq. (III.1) with  $\mu$  and  $\nu$  summed:

$$G_{N\mu\nu} = \frac{-ig_{\mu\nu}}{M} \left( \frac{g^2}{8\pi^2} \right)^N \int_0^\infty \frac{d\Omega (M^2 d_{1N} + p \cdot q C')}{C^3} \exp\left(\frac{iD}{C}\right) \quad (\text{III.8})$$

where  $\gamma_1 = \gamma_2 = \dots \gamma_N = 0$ . From the above calculation it is evident that the part of  $G_{N\mu\nu}$  corresponding to  $p \cdot q C'$  will dominate the leading part of  $G_{N\mu\nu}$  by a factor of  $q \cdot p / M^2$  compared to the  $M^2 d_{1N}$  part of the  $G_{N\mu\nu}$  integral. The relative factor of  $\rho$  is due to the suppression of the leading pole from  $\eta = -1$  to  $\eta = -2$  by the  $d_{1N}$  factor in eq. (III.5). This factor of  $q \cdot p \rho$  is the only difference between the two calculations. Therefore the leading contribution to  $T_{N\mu\nu}$  coming from the term,  $-g_{\mu\nu}(q+k_1) \cdot p P_N^b$ , is

$$\frac{-g_{\mu\nu} q \cdot p}{M|q^2|\rho(N!)^2} \left( \frac{g^2 K_1 \ln|q^2| \ln \rho}{8\pi^2} \right)^N = \frac{g_{\mu\nu}}{2M(N!)^2} \left( \frac{g^2 \ln|q^2| \ln \rho N}{8\pi^2} \right) \quad (\text{III.9})$$

The contributions of the remaining terms in  $P_N$  to  $T_{N\mu\nu}$  will not be relevant to the leading logarithmic behavior of  $T_{1N}$  and  $T_{2N}$ . They will be at least a factor of  $\ln \rho$  below the lead-

ing logarithms given in eqs. (III.7) and (III.9) and can therefore be ignored under the assumptions that  $|q^2|$  and  $\omega$  are large enough to make this approximation valid. (It should be noted that  $C' = \prod_{j=1}^N (\alpha_j + \beta_j)$  in eq. (III.5) due to the scalings and delta functions. Consequently the integral can be shown to be exactly equal to  $(n+2)^{-N}$ . Thus the  $\rho$  behavior of this integral could be found exactly without recourse to the leading logarithm approximation.)

Now we evaluate the contributions to the leading behavior of  $T_{N\mu\nu}$  from the terms  $(q+k_1)_\mu \sum_{j=1}^N k_{j\nu} \tilde{p}_N^j + (q+k_1)_{\nu} \sum_{j=1}^N k_{j\mu} \tilde{p}_N^j + g_{\mu\nu} [MP_N^a - (q+k_1)_\mu \sum_{j=1}^N k_{j\nu} \tilde{p}_N^j]$ . The first term we consider is  $(q+k_1)_\nu \sum_{j=1}^N k_{j\mu} \tilde{p}_N^j$ . According to Appendix A  $\tilde{p}_N^j$  has the form:

$$\tilde{p}_N^j = 2^{j-1} \prod_{r=1}^{j-1} (k_r^2 - M^2) \sum_{s=0}^{N-j} \{e\}^j B_{e_1}^{e_1} B_{e_1}^{e_2} \dots B_{e_s}^{N+1}$$

with  $\{e\} = \{e_1, e_2, \dots, e_s\}$ ,  $j < e_1 < e_2 < \dots < e_s \leq N$  and

$$B_i^j = 2(4^{j-i} M^2 - 2^{j-i} k_i \cdot k_j) \prod_{r=i+1}^{j-1} (k_r^2 - M^2).$$

Since we are interested in the leading behavior of  $T_{N\mu\nu}$  we approximate  $B_i^j$  by

$$B_i^j \sim -2^{j+1-i} k_i \cdot k_j \prod_{r=i+1}^{j-1} (k_r^2 - M^2) \quad (\text{III.10})$$

and as a result we obtain an expression for  $\tilde{p}_N^j$  which is exact to leading order:

$$\tilde{p}_N^j \rightarrow 2^N \prod_{i=1}^N (k_i^2 - M^2) \sum_{s=0}^{N-j} (-2)^{s+1} \sum_{\{e\}} \frac{k_j \cdot k_{e_1} k_{e_1} \cdot k_{e_2} \dots k_{e_{s-1}} \cdot k_{e_s} k_{e_s} \cdot p}{(k_j^2 - M^2)(k_{e_1}^2 - M^2) \dots (k_{e_s}^2 - M^2)}$$

Following the same procedure as in the calculations just concluded we introduce and use derivatives with respect to  $\gamma_i$  for  $i \notin e$  and  $i \neq j$  to do the corresponding integrations, and of the  $N_i$  only keep the parameters,  $\gamma_j, \gamma_e, \gamma_{e_2}, \gamma_{e_3}, \dots, \gamma_{e_s}$ . Therefore, with all  $\gamma_i$  equal to zero but these, we obtain the following contribution to  $T_{N\mu\nu}$

$$H_{N\mu\nu} = \frac{i}{M} \left( \frac{g^2}{8\pi^2 i} \right)^N \sum_{j=1}^N \sum_{s=0}^{N-j} i^{N-s-1} (-2)^{s+1} \sum_{\{e\}0}^{\infty} \frac{d\Omega}{C^2}.$$

$$\cdot [(q+k_1)_\nu k_{j\mu} k_j \cdot k_{e_1} k_{e_1} \cdot k_{e_2} \dots k_{e_s} \cdot p \exp \left( \frac{iD(A)}{C} \right)]_{A_0=A_1=\dots=0}$$

where it is understood that the loop momenta in the intrgeal represent derivative operators. The derivative represented by  $(q+k_1)_\nu$  is  $(2i\alpha_0)^{-1} \frac{\partial}{\partial A_0^\nu}$  and use of eq. (III.1) for the remaining  $s+1$  pairs of derivatives leads to the following derivative expression

$$(q+k_1)_\nu k_{j\mu} k_j \cdot k_{e_1} \dots k_{e_{s-1}} \cdot k_{e_s} k_{e_s} \cdot p \rightarrow \frac{(-1)^{s+1} p^\lambda}{(2i)^{s+1} z_{e_0} z_{e_1} \dots z_{e_s}}.$$

$$\cdot \sum_{m=0}^{s+1} \sum_{\{v\}} \frac{(-1)^m}{(2i)^{m+1} z_{e_{v_1}} z_{e_{v_2}} \dots z_{e_{v_m}} \alpha_0}.$$

$0 \leq v_1 < v_2 < \dots < v_m \leq s$

$$\frac{\partial^{2M+1}}{\partial A_0^{\nu} \partial A_{e_{v_1}}^{\mu} \partial A_{e_{v_1}}^{\nu_1} \partial A_{e_{v_2}}^{\nu_2} \partial A_{e_{v_2}}^{\nu_2} \partial A_{e_{v_3}}^{\nu_3} \partial A_{e_{v_{m-1}}}^{\nu_{m-1}} \partial A_{e_{v_m}}^{\nu_{m-1}} \partial A_{e_{v_m}}^{\lambda}}.$$

where we have expanded the factors and summed over the indices of the  $g_{\alpha\beta}$  which appear. We have also let  $e_0 = j$  and  $Z_i = \beta_i + \gamma_i$ . The  $m = 0$  term in the sum is

$$\frac{(-1)^{s+1} p_\mu}{(2i)^{s+2} \alpha_0 Z_{e_0} Z_{e_1} \dots Z_{e_s}} \frac{\partial}{\partial A_0^v}.$$

We have applied these  $(2m+1)$  order derivatives to  $\exp(iD(A)/C)$  in Appendix C and found that the part of the resulting polynomials that gave contributions to the leading behavior of the  $p_\mu p_\nu$  part of  $T_{N\mu\nu}$  is (eq. (C10))

$$p_\mu p_\nu \sum_{h=0}^m \left(\frac{2i}{C}\right)^{2m+1-h} (-1)^{mf(m,h)} d_{1N} (d_{0N}^{p,q})^{m-h} \prod_{i=1}^m C_{e_{v_i}-1}^0 C_N^{e_{v_i}} \quad (\text{III.11})$$

where  $f(m,h)$  is an integer and  $C_j^i$  is a Feynman parameter polynomial defined in Appendix B. After substitution of these expressions into  $H_{N\mu\nu}$  we obtain:

$$H_{N\mu\nu} \rightarrow \frac{ip_\mu p_\nu}{M} \left(\frac{g^2}{8\pi^2}\right)^N \sum_{j=1}^N \sum_{s=0}^{N-j} (-1)^{s+1} \sum_{\{e\}} \sum_{m=0}^{s+1} \sum_{\{v\}} \sum_{h=0}^m (2ip \cdot q)^{m-h} \cdot f(m,h) \mathcal{L}_{\{e\}\{v\}}^{Nsmh} \quad (\text{III.12})$$

with

$$\mathcal{L}_{\{e\}\{v\}}^{Nsmh} = \int_0^\infty \frac{d\Omega \exp\left(\frac{iD}{C}\right) d_{1N} (d_{0N})^{m-h}}{C^{2m+3-h} Z_{e_0} Z_{e_1} \dots Z_{e_s}} \prod_{r=1}^m Z_{e_{v_r}} C_{e_{v_r}-1}^0 C_N^{e_{v_r}} \quad (\text{III.13})$$

The calculation of the asymptotic behavior in  $|q^2|$  for fixed  $\rho$  of the integral in eq. (III.13), and then the leading  $\rho$  behavior is similar to the calculations done previously. The Mellin transform in  $|q^2|$  of  $\mathcal{L}_{\{e\}\{v\}}^{\text{Nsmh}}$  is

$$\tilde{\mathcal{L}}_{\{e\}\{v\}}^{\text{Nsmh}} = i^{\eta} \Gamma(-\eta) \int_0^\infty \frac{d\Omega d_{1N}^{m-h+1} \alpha_0^{m-h+\eta} (\rho d_{1N} + C')^\eta e^{iJ} U}{Z_{e_0} Z_{e_1} \dots Z_{e_s} C^{2m+3-h+\eta}}$$

where

$$U = \prod_{r=1}^m Z_{e_{v_r}} C_{e_{v_r}-1}^0 C_N^{e_{v_r}}$$

If we scale as in eqns. (III.3), modifying the scaling to include the  $\gamma_{e_i}$  for  $i = 0, 1, 2, \dots, s$

$$\gamma_{e_i} = x_{e_i} x_{e_i+1} \dots x_N \tilde{\gamma}_{e_i}$$

and including  $\tilde{\gamma}_{e_i}$  in the appropriate  $\delta$ -functions, then we obtain

$$\begin{aligned} \tilde{\mathcal{L}}_{\{e\}\{v\}}^{\text{Nsmh}} = i^{\eta} \Gamma(-\eta) \int_0^1 d\tilde{\Omega} \int_0^\infty \frac{dx_1 \dots dx_N d_{1N}^{m-h+1} (\tilde{\alpha}_0 x_1 x_2 \dots x_N)^{m-h+\eta}}{\tilde{Z}_{e_0} \tilde{Z}_{e_1} \dots \tilde{Z}_{e_s} \tilde{C}^{m+3-h+\eta}} \cdot \\ \cdot (\rho \tilde{d}_{1N} + \tilde{C}')^\eta e^{iJ} \tilde{U} \delta(1 - \tilde{\alpha}_0 - \tilde{\alpha}_1 - \tilde{\beta}_1) \dots \end{aligned}$$

Partially integrating with respect to  $\tilde{\alpha}_0, x_1, x_2, \dots, x_N$  gives a pole of order  $N+1$  at  $\eta = h-m-1$ . This implies the leading  $|q^2|$  behavior ( $\rho$  fixed) is



$$\mathcal{L}_{\{e\}\{v\}}^{Nsmh} \rightarrow \frac{\Gamma(m+1-h) (\ln|q^2|)^N}{(i|q^2|)^{m+1-h} N!} \cdot \int_0^1 \frac{d\tilde{\Omega}' \tilde{d}_{1N}^{m-h+1} \tilde{U} \delta(1-\tilde{\alpha}_1-\tilde{\beta}_1) \dots \delta(1-\tilde{\alpha}_{e_i}-\tilde{\beta}_{e_i}-\tilde{\gamma}_{e_i}) \dots}{\tilde{z}_{e_0} \dots \tilde{z}_{e_s} \tilde{C}'^{m+2} (\rho \tilde{d}_{1N} + \tilde{C}')^{m+1-h}} \quad (III.14)$$

after evaluating the residue at  $\eta=h-m-1$ .

We now investigate the  $|\rho| \gg 1$  behavior of the remaining Feynman parameter integral in eq. (III.14). The Mellin transform in  $\rho$  is<sup>16</sup>

$$\frac{\Gamma(m+1-h)}{N! (i|q^2|)^{m+1-h}} (\ln|q^2|)^N (-1)^{m-h} [-\pi \csc(\pi\eta)] \binom{-\eta-1}{m-h} \cdot \int_0^1 \frac{d\Omega' d_{1N}^{m-h+1+\eta} U \delta(1-\alpha_1-\beta_1) \dots}{z_{e_0} z_{e_1} \dots z_{e_s} C'^{2m+3-h+\eta}}$$

Partially integrating  $\alpha_1, \alpha_2, \dots, \alpha_N$  exhibits a pole at  $\eta=h-m-2$  of order  $N+1$  (counting the pole due to  $\csc(\pi\eta)$ ). This is the leading pole which results in an eventual contribution to the absorptive part of  $T_{N\mu\nu}$ . The leading behavior is

$$\mathcal{L}_{\{e\}\{v\}}^{Nsmh} \rightarrow \frac{-(m+1-h)! (\ln|q^2| \ln \rho)^N}{(i|q^2|\rho)^{m-h} i|q^2|\rho^2 (N!)^2} K_1^{N-s-1} K_2^{s+1}$$

with  $K_1$  given by eq. (III.6) and

$$K_2 = \int_0^1 \frac{d\beta d\gamma \delta(1-\beta-\gamma)}{(\beta+\gamma)^2} \quad (III.15)$$

The factors of  $K_2$  come from the  $s+1$   $\gamma_{e_i}$  which occurred in this

calculation. There was a pole at  $\eta=h-m-1$  of first order due to  $\csc(\pi\eta)$  which we ignored since that term does not lead to a contribution to the absorptive part of  $T_{N\nu\mu}$ .

If we put the last expressions and eq. (III.12) together we obtain the leading behavior of the  $p_\mu p_\nu$  part of

$(q + k_1)_\nu \sum_\mu k_{j\mu} \tilde{p}_N^j + (q+k_1)_\mu \sum_\nu k_{j\nu} \tilde{p}_N^j$ , namely,

$$\frac{-2 p_\mu p_\nu}{M|q^2|\rho^2(N!)} \left( \frac{g^2 K_1 \ln|q^2| \ln \rho}{8 \pi^2} \right) \sum_{j=1}^N \sum_{s=0}^{N-j} \left( \frac{-2}{K_1} \right)^{s+1} \binom{N-j}{s} \sum_{m=0}^{s+1} \binom{s+1}{m} \sum_{h=0}^m (-1)^{m-h} (m-h+1)! \cdot f(m,h) \quad (III.16)$$

where the sum over  $\{e\}$ , such that  $j < e_1 < e_2 < \dots e_s \leq N$ , was replaced by  $\binom{N-j}{s}$  which counts the number of these (identical) terms, the sum over  $\{v\}$  was replaced by  $\binom{s+1}{m}$  for similar reasons, and we used  $2 p \cdot q = -|q^2|\rho$ . In Appendix C we prove that

$$\sum_{h=0}^m (-1)^h (m-h+1)! f(m,h) = 1$$

for all  $m$ . Substituting this into eq. (III.16) and noting

$$\sum_{m=0}^{s+1} \binom{s+1}{m} (-1)^m = (1-1)^{s+1} = 0$$

proves that the numerical coefficient is zero and that these terms so not contribute to the leading behavior of the  $p_\mu p_\nu$  part of  $T_{N\mu\nu}$ .

We now find the leading behavior coming from  $-g_{\mu\nu}(q+k_1)$ .  
 $\sum_{j=1}^N k_j \tilde{p}_N^j$ . The calculation proceeds in the same manner as the

previous calculation. However the polynomial resulting from applying derivatives to  $\exp(iD(A)/C)$  has a different leading part. Instead of having the leading part given by eq. (III.11) we now have the expression given by eq. (C13)

$$\sum_{h=0}^{m-1} \left(\frac{2i}{C}\right)^{2m+1-h} (-1)^m p.q C'(d_{0N} p.q)^{m-h} f_1(m,h) \prod_{i=1}^m C_{v_i}^0 C_{v_i}^{-1} C_N^e .$$

with  $f_1(m,h)$  an integer.

The calculation with this expression is virtually unchanged from the above except for the pole being shifted one unit to the right when the  $|\rho| \gg 1$  behavior is being found. Thus the contribution of this term is

$$\frac{1}{2M(N!)^2} \left( \frac{g^2 K_1 \ln|q^2| \ln \rho}{8 \pi^2} \right)^N \sum_{j=1}^N \sum_{s=0}^{N-j} \left( \frac{-K_2}{K_1} \right)^{s+1} \binom{N-j}{s} \sum_{m=0}^{s+1} \binom{s+1}{m} (-1)^m .$$

$$\cdot \sum_{h=0}^{m-1} (-1)^h (m-h)! f_1(m,h)$$

In Appendix C we prove

$$\sum_{h=0}^m (-1)^h (m-h)! f_1(m,h) = 1$$

and as a result the numerical coefficient is zero. Thus there is no contribution to leading order from these terms.

Finally, a calculation similar to the above for the leading part of the  $g_{\mu\nu} p_N^a$  term shows that it is a factor on  $\ln|q^2|$  less than that of eq. (III.9) and thus does not contribute to leading order. There is also a part of  $(q+k_1)_\nu \sum k_{j\mu} \tilde{p}_N^j$  pro-

portional to  $g_{\mu\nu}$  (after performing derivatives of  $\exp(iD(A)/C)$ ) which is a factor of  $\ln|q^2|$  less than that of eq. (III.9).

In conclusion, the leading logarithmic contribution of the  $N+1$  rung ladder diagram is

$$W_{1N} \sim \frac{1}{2^M \ln \omega N! (N-1)!} \left( \frac{g^2 \ln|q^2| \ln \omega}{8 \pi^2} \right)^N \quad (\text{III.17})$$

$$2M W_{1N} = \omega \nu W_{2N} \quad (\text{III.18})$$

from eqs. (III.7) and (III.9). Upon summation over  $N$  we obtain eqs. (I.21a) and (I.19b).

### C. The Neutral Pseudoscalar Meson Model

The neutral vector meson model we have just studied in section III.B is closely related to a neutral pseudoscalar meson model. The interaction Lagrangian for this model is

$$- : e \bar{\psi} \gamma_\mu \psi A^\mu : - : i g \bar{\psi} \gamma_5 \psi \phi :$$

with  $\phi$  the pseudoscalar meson field and  $\psi$  the nucleon field. Pseudoscalar mesons will now be exchanged on the dashed lines of the diagram in Fig. (II.1). All remains the same as in the neutral vector meson model except that one replaces each  $\gamma_{\alpha_i}$  with a  $\gamma_5$  in the expression for  $P_N$  given in eq. (A1). As a result  $P_N$  has the solution given in eqs. (A27) through eq. (A30). If we are only interested in the leading logarithmic behavior we can set  $M=0$  throughout  $P_N$ . A comparison of  $P_N$  in the two models

with  $M=0$  shows that  $P_N$  in the neutral vector meson theory is a factor of  $2^N$  greater than  $P_N$  in the neutral pseudoscalar meson theory. Consequently we can use eqs. (III.17) and (III.18) to obtain the contribution of the  $N+1$  rung diagram in the neutral pseudoscalar meson model:

$$2M W_{1N} = \omega v W_{2N} \quad (\text{III.19})$$

$$W_{2N} = \frac{2M}{|q^2| \omega^2 1n\omega N!(N-1)!} \left( \frac{g^2 1n|q^2| 1n\omega}{16 \pi^2} \right)^N \quad (\text{III.20})$$

Summing over  $N$  gives eqs. (I.19b) and (I.22).

#### D. Truss Bridge Diagram Model

In this section we will study a model in which the inelastic structure functions have forms which are intermediate between those in chapter II's models and those in the models studied earlier in this chapter. All particles in this model are spinless except the photon which is spin one. The interaction Lagrangian is

$$g\psi^*\psi\phi + G\psi^*\psi\phi^2 - ie\psi^*\overleftrightarrow{\partial}_\mu\psi A^\mu \quad (\text{III.21})$$

with  $\psi$  the nucleon field,  $A^\mu$  the electromagnetic field and  $\phi$  a meson field. In this model we sum the leading logarithms of all diagrams of the form of Fig. (III.3) and its mirror image. They are called truss bridge diagrams.

The Feynman integral corresponding to Fig. (III.3) and the mirror image can be put in the form of eq. (II.1) if

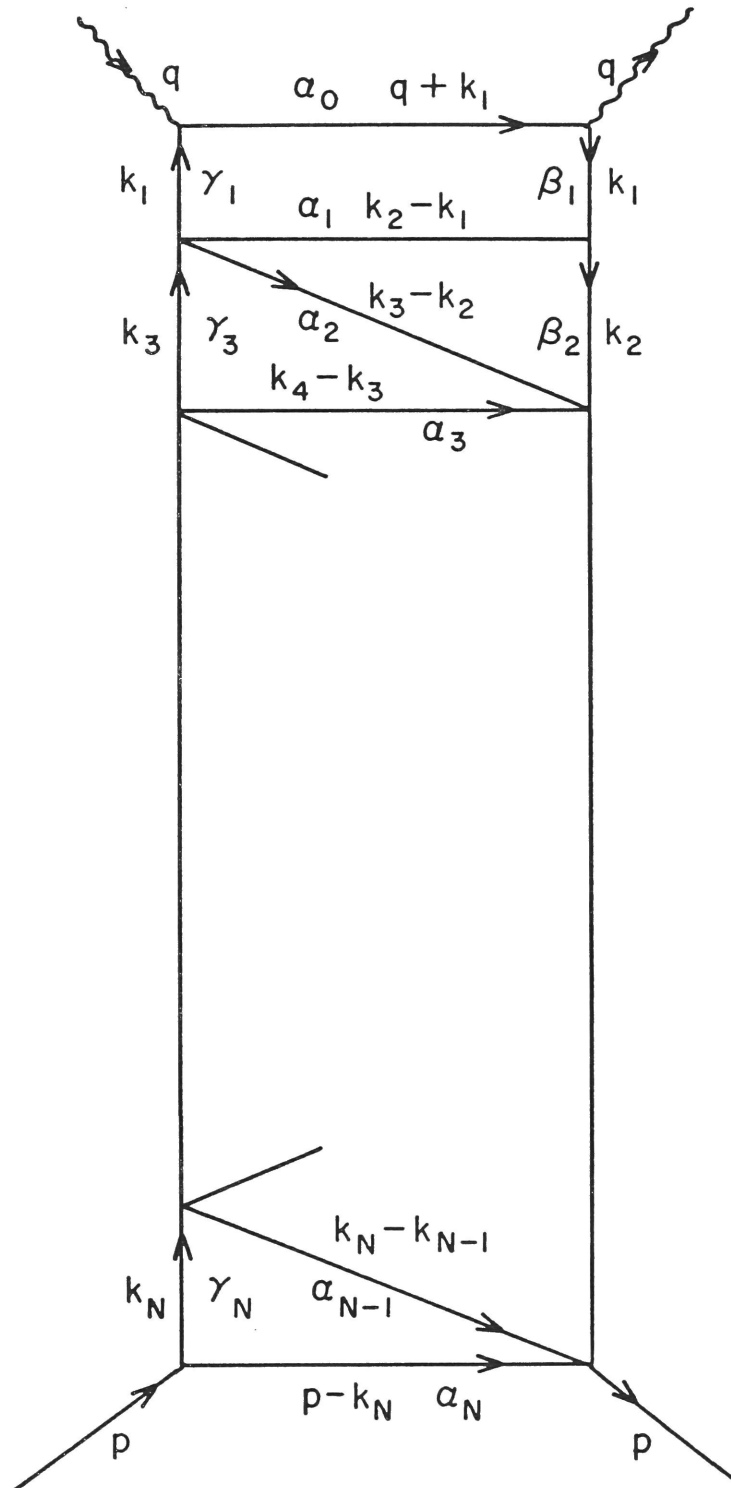


Fig. III.3. A Truss Bridge Diagram

$$\mathcal{N}_{N\mu\nu} = 2g^2(iG)^{N-1}(2k_1+q)_\mu(2k_1+q)_\nu \prod_{j=2}^N [i^{-1}(k_j^2-M^2)]$$

where  $iG$  is associated with each four particle vertex, a factor of 2 was introduced to take account of the equality of the diagram and its mirror image and where we have introduced factors to compensate for similar factors occurring in the denominator of the integral.  $\mathcal{N}_{N\mu\nu}$  can be rewritten so that it is independent of loop momenta. We introduce the dummy momenta  $A_0$  and  $A_1$  and follow the procedure of section II.C. Therefore  $(2k_1+q)_\mu(2k_1+q)_\nu$  is replaced with

$$\frac{4}{(2i)^2\alpha_0(\beta_1+\gamma_1)} \frac{\partial^2}{\partial A_0^\nu \partial A_1^\mu}$$

which results in the correct expression for the  $p_\mu p_\nu$  and  $g_{\mu\nu}$  parts of  $T_{N\mu\nu}$  though not for the  $q_\mu$  or  $q_\nu$  dependent parts. The factors  $\prod_{j=2}^N (k_j^2-M^2)$  can be replaced with

$$\frac{1}{i^{N-1}} \prod_{j=2}^N \frac{\partial}{\partial \gamma_j} \quad (\text{III.22a})$$

or

$$\frac{1}{i^{N-1}} \frac{\partial^{N-1}}{\partial \gamma_2 \partial \beta_3 \partial \gamma_4 \partial \beta_5 \dots} \quad (\text{III.22b})$$

Therefore  $T_{N\mu\nu}$  is

$$T_{N\mu\nu} = \frac{(-\sigma)^{N-1}g^2}{8\pi^2} \int \frac{d\Omega}{\alpha_0(\beta_1+\gamma_1)} \prod_{j=2}^N \frac{\partial}{\partial \gamma_j} \frac{\partial^2}{\partial A_0^\nu \partial A_1^\mu} \left( \frac{e^{iD/C}}{C^2} \right) \Bigg|_{A_0=A_1=0} \quad (\text{III.24})$$

where  $\sigma = G/16\pi^2$ ,  $C$  is given by eq. (B4) and  $D$  is given by eq. (B6) with  $A_2 = A_3 = \dots = A_N = 0$ .

After performing the derivatives with respect to  $A_0$  and  $A_1$   $T_{N\mu\nu}$  is

$$T_{N\mu\nu} \equiv \frac{-g^2(-\sigma)^{N-1}}{2\pi^2} \int d\Omega \prod_{j=2}^N \frac{\partial}{\partial \gamma_j} \left[ \left\{ \frac{d_{1N}^2}{C^2} p_\mu p_\nu - \frac{C_{N\mu\nu}^1}{2iC} \right\} \frac{e^{iD/C}}{C^2} \right] \quad (\text{III.25})$$

if we ignore terms proportional to  $q_\mu$  and  $q_\nu$ . Therefore

$$T_{1N} = \frac{-g^2(-\sigma)^{N-1}}{2\pi^2} \int d\Omega \prod_{j=2}^N \frac{\partial}{\partial \gamma_j} \left[ \frac{C_N^1}{2iC^3} e^{iD/C} \right] \quad (\text{III.26})$$

and

$$T_{2N} = \frac{-g^2 M^2 (-\sigma)^{N-1}}{2\pi^2} \int d\Omega \prod_{j=2}^N \frac{\partial}{\partial \gamma_j} \left[ \frac{d_{1N}^2}{C^4} e^{iD/C} \right] \quad (\text{III.27})$$

We first evaluate the leading logarithmic behavior of  $T_{1N}$  in  $|q^2|$  with  $\omega$  fixed. After using the derivatives to perform the integrations over  $\gamma_2, \gamma_3, \dots, \gamma_N$  and Mellin transforming in  $|q^2|$  we obtain

$$\tilde{T}_{1N} = \frac{-g^2 \sigma^{N-1}}{4i\pi^2} \int \frac{d\Omega C_N^1}{C^{3+\eta}} \alpha_0^\eta (\rho d_{1N} + C')^\eta e^{iJ_1 \eta} \Gamma(-\eta) \quad \text{Re} \eta < 0 \quad (\text{III.28})$$

where it is understood that  $\gamma_2 = \gamma_3 = \dots = \gamma_N = 0$  in all expressions in the equation. (Only the lower bounds of the integrations over  $\gamma_2, \dots, \gamma_N$  give a non-zero contribution.)

The leading pole at  $\eta = -1$  is of order  $N+1$ . To make this explicit we perform the scaling given in eq. (III.3) with this modification: let  $\tilde{\beta}_1$  be replaced with  $\tilde{\beta}_1 + \tilde{\gamma}_1$  throughout the



set of scaling equations and perform the following scaling of  $\gamma_1$

$$\gamma_1 = x_1 x_2 \dots x_N \tilde{\gamma}_1.$$

We follow the same procedure as we did between eqs. (III.3) and eq. (III.4). The result is

$$T_{1N} \sim \frac{g^2 \sigma^{N-1} (\ln|q^2|)^N}{4\pi^2 |q^2| N!} \int \frac{d\Omega' C_N^1 (1-\alpha_1-\beta_1-\gamma_1) \delta(1-\alpha_2-\beta_2) \dots \delta(1-\alpha_N-\beta_N)}{C'^2 (\rho d_{1N} + C')} \quad (\text{III.29})$$

where due to scalings,  $C' = (\alpha_1 + \beta_1 + \gamma_1) C_N^1$  and  $C_N^1 = \prod_{j=2}^N (\alpha_j + \beta_j)$ . Taking account of the delta functions allows us to perform the integrations over all parameters except  $\alpha_1, \alpha_2, \dots, \alpha_N$  and we obtain

$$T_{1N} \sim \frac{g^2 \sigma^{N-1} (\ln|q^2|)^N}{4\pi^2 |q^2| N!} \int_0^1 \frac{d\alpha_1 d\alpha_2 \dots d\alpha_N}{\rho d_{1N} + 1} \quad (\text{III.30})$$

which is the leading logarithmic behavior in  $|q^2|$  for fixed  $\omega$ .

The integral in eq. (III.30) can be performed exactly. The simplest way is to Mellin transform the integral in  $\rho$  which is

$$-\pi \csc(\pi\eta) \int_0^1 d\alpha_1 d\alpha_2 \dots d\alpha_N d_{1N}^\eta = \frac{-\pi \csc \pi\eta}{(\eta+1)^N}$$

The inverse Mellin transform of this function is

$$\frac{(\ln \rho)^N}{N! \rho} = \frac{1}{\rho^2} + \frac{1}{\rho^3} - \frac{1}{\rho^4} + \dots$$

Only the first term contributes to the absorptive part of  $T_{1N}$ . Therefore if we take the imaginary part of  $T_{1N}$  in eq. (III.30) and use eq. (I.16a) we obtain

$$W_{1N} \sim \frac{g^2 \ln|q^2|}{4\pi^2 \omega |q^2| N! (N-1)!} (\sigma \ln|q^2| \ln \omega)^{N-1} \quad (\text{III.31})$$

which gives eq. (I.24) upon summation over  $N$ . Note that eq. (III.31) gives the leading logarithmic behavior of  $T_{1N}$  in  $|q^2|$  for any (fixed) value of  $\omega$ .

Next we evaluate the leading behavior of  $T_{2N}$ . It will be more convenient to use the derivative expression in eq. (III.22b) rather than (III.22a). Therefore eq. (III.27) becomes

$$T_{2N} = \frac{-g^2 M^2}{2\pi^2} (-\sigma)^{N-1} \int d\Omega \frac{\partial^{N-1}}{\partial \gamma_2 \partial \beta_3 \partial \gamma_4 \dots} \left\{ \frac{d_{1N}^2}{C^4} e^{iD/C} \right\} \quad (\text{III.32})$$

After performing the integrations over  $\gamma_2, \beta_3, \dots$  we obtain

$$T_{2N} = \frac{-g^2 M^2 \sigma^{N-1}}{2\pi^2} \int \frac{d\Omega d_{1N}^2}{C^4} e^{iD/C} \quad (\text{III.33})$$

where it is understood that  $d\Omega = d\alpha_0 d\beta_1 d\gamma_1 d\alpha_1 d\alpha_2 \dots d\alpha_N d\beta_2 d\gamma_3 d\beta_4 \dots$  and  $\gamma_2 = \beta_3 = \gamma_4 = \dots = 0$  throughout the integral. The evaluation of the leading logarithmic term in  $|q^2|$  is exactly the same as the evaluation in section II.B. Scalings do not contribute to the leading logarithmic term. Therefore the leading term is

$$T_{2N} \sim \frac{-g^2 M^2 \sigma^{N-1}}{2i\pi^2 |q^2|} \int \frac{d\Omega' d_{1N}^2 e^{iJ'}}{C'^3 (\rho d_{1N} + C')} \quad (\text{III.34})$$

We will now assume  $\rho$  is very large and find the leading logarithmic behavior in  $\rho$  of the integral in eq. (III.34). The Mellin transform in  $\rho$  is

$$\tilde{T}_{2N} \sim \frac{-g^2 M^2 \sigma^{N-1}}{2i\pi^2 |q^2|} (-\pi \csc \pi \eta) \int \frac{d\Omega' d_{1N}^{2+\eta}}{C'^{4+\eta}} e^{iJ'} \quad (\text{III.35})$$

We can infer the leading  $\eta$  pole behavior of

$$I_N(\eta) = \int \frac{d\Omega' e^{iJ'}}{C'^{4+\eta}} d_{1N}^{2+\eta} \quad (\text{III.36})$$

from the work of Bjorken and Wu.<sup>18</sup> Rewriting eq. (III.36) in terms of their notation we obtain:

$$I_N(\eta) = kA(\eta+2, N-1, 0) \quad (\text{III.37})$$

where

$$A(\eta, N-1, p) = \int_0^1 \frac{d\Omega'' d_{1N}^\eta}{C''^{2+\eta}} \left[ \ln \left( \frac{C''}{\alpha_N (C'' - \alpha_N \frac{C_0''}{C_{N-1}''})} \right) \right]^p \quad (\text{III.38})$$

and the double primes indicate that  $\alpha_0, \beta_1$  and  $\gamma_1$  have been set equal to zero in those expressions and  $d\beta_1 d\gamma_1 d\Omega'' = d\Omega'$ . To calculate  $k$  we evaluate  $I_1(\eta)$  and  $A(\eta+2, 0, 0)$ :

$$I_1(\eta) = \frac{1}{iM^2} \frac{1}{\eta+3}$$

$$A(\eta+2, 0, 0) = \int_0^1 d\alpha_1 \alpha_1^{\eta+2} = \frac{1}{\eta+3}$$

and use eq. (III.37) to obtain  $k = (iM^2)^{-1}$ . From Bjorken and Wu we have

$$A(\eta, N, 0) = \frac{(2N)!}{N!(N+1)!(\eta+1)^{2N+1}}$$

and therefore

$$I_N(\eta) \sim \frac{1}{iM^2} \frac{(2N-2)!}{N!(N-1)!(\eta+3)^{2N-1}} \quad (\text{III.39})$$

Thus the inverse Mellin transform of the leading pole of eq. (III.35) is

$$T_{2N} \sim \frac{g^2 \sigma^{N-1} (1n\rho)^{2N-1}}{2\pi^2 |q^2| \rho^3 N! (N-1)! (2N-1)}$$

and

$$W_{2N} \sim \frac{g^2 (\sigma^{1/2} 1n\omega)^{2N-2}}{2\pi^2 |q^2| \omega^3 N! (N-1)!}$$

Summing over  $N$  results in eq. (I.23).

## CHAPTER IV

Comments on the Spin One-Half Nucleon Models

## A. The Leading Behavior of Non-Ladder Diagrams

In the spin one-half nucleon models we studied in the last chapter we only included ladder graphs with mesons exchanged on the ladders' rungs. There are many other graphs contributing to the virtual Compton amplitude in each order of  $g$ , the meson-nucleon coupling constant, in the pseudoscalar meson and neutral vector meson field theories. In this section we consider these graphs to fourth order in  $g$ . We show ladder graphs have a leading logarithmic behavior which dominates the leading logarithmic behavior of all other graphs in each order of  $g$  to order  $g^4$ . This suggests that there is no cancellation of the leading logarithms calculated in our models by the leading logarithms of non-ladder graphs.

We will show that there is a set of ladder graphs containing nucleon loops (cf. Fig. IV.3) having the same leading logarithmic behavior as the ladder graphs (without nucleon loops) in our neutral vector meson model. However, ladder graphs with nucleon loops in the pseudoscalar meson theory do not have the same leading logarithmic behavior as ladder graphs (without nucleon loops) in our pseudoscalar meson model. This is the only qualitative difference between the pseudoscalar meson theory calculation of the Compton amplitude and the neutral vector meson theory calculation so far as leading logarithms is concerned. It is interesting to

note that the leading logarithm calculations of the nucleon electromagnetic vertex in a pseudoscalar meson model (by Appelquist and Primack<sup>19</sup>) and in a neutral vector meson model (by Jackiw<sup>20</sup>) are radically different. They differ because the leading logarithms in the pseudoscalar meson calculation come from the ultraviolet region of the loop integrations while the leading logarithms in the neutral vector meson theory come from the infrared region. In the case of the forward Compton amplitude the leading logarithms come from the infrared region in both theories.

In his calculation of the electromagnetic vertex function Jackiw showed that ladder diagrams with crossed rungs had the same leading logarithmic behavior as ladders with uncrossed rungs. We will now show that the analogous statement is not true for the virtual Compton amplitude by calculating the contribution of the diagram shown in Fig. (IV.1) to  $T_{\mu}^{\mu}$  in the neutral vector meson theory.

We follow the procedure outlined in Chapter II and find the contribution to  $T_{\mu}^{\mu}$  is

$$I = \frac{-16i}{M} \left( \frac{g^2}{16\pi^2} \right)^2 \int \frac{d\Omega \mathcal{G} e^{iD/C}}{C^2} \quad (\text{IV.1})$$

with

$$C = (\alpha_0 + \beta_1 + \gamma_1)(\alpha_1 + \alpha_2 + \beta_2 + \gamma_2) + (\alpha_1 + \beta_2)(\alpha_2 + \gamma_2)$$

$$D = \alpha_0 q^2 [\rho(\alpha_1 \alpha_2 - \beta_2 \gamma_2) + C'] + JC$$

$$\mathcal{G} = [k_1 \cdot p k_1 \cdot (k_1 + 2q) - k_1^2 p \cdot q] k_2 \cdot (p - k_2 + k_1)$$

$$= \left[ \frac{1}{2i} \left( \frac{\partial}{\partial \beta_2} + \frac{\partial}{\partial \gamma_2} - \frac{\partial}{\partial \alpha_1} - \frac{\partial}{\partial \alpha_2} \right) \left( \frac{1}{i} \frac{\partial}{\partial \alpha_0} - q^2 \right) - \frac{p \cdot q}{i} \frac{\partial}{\partial \gamma_1} \right] \cdot \frac{1}{2i} \left( \frac{\partial}{\partial \beta_1} - \frac{\partial}{\partial \alpha_1} - \frac{\partial}{\partial \alpha_2} \right)$$

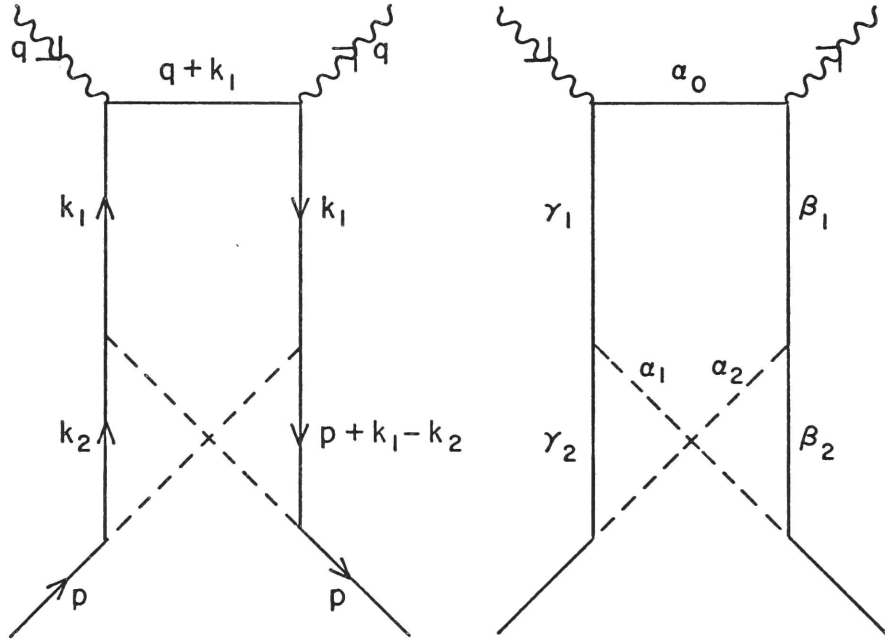


Fig. IV.1. Diagrams With Crossed Rungs

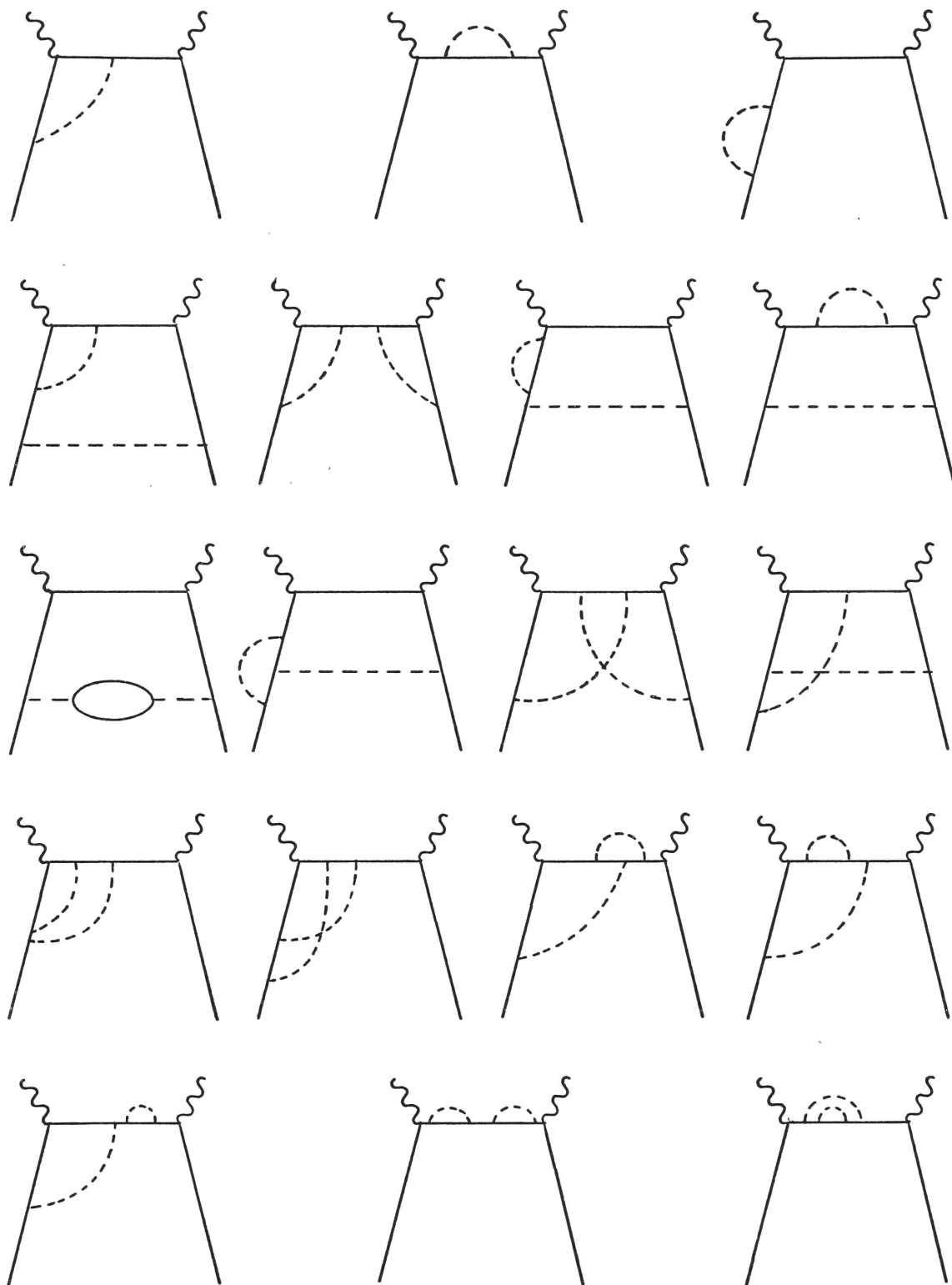


Fig. IV.2. Some Compton Amplitude Diagrams.



where  $\mathcal{O}$  is written both in terms of its original loop momenta and also in terms of derivatives with respect to Feynman parameters. The validity of the operator expression for  $\mathcal{O}$  is easily seen at the stage of this calculation corresponding to eq. (II.3).

After examining the leading logarithmic behavior in the same manner as previously we find that terms in  $\mathcal{O}$  containing derivatives with respect to  $\alpha_0, \alpha_1$  or  $\alpha_2$  lead to no  $q^2$  dependent contribution to the absorptive part and are properly ignored. The leading logarithm of the term corresponding to  $\partial^2/\partial\beta_1\partial\gamma_1$  is a factor of  $\ln\omega$  less than the  $g^4$  order ladder graph with uncrossed rungs and the leading logarithm of the terms  $\frac{\partial^2}{\partial\beta_2\partial\beta_1}$  and  $\frac{\partial^2}{\partial\gamma_2\partial\beta_1}$  is a factor of  $\ln|q^2|$  less. Consequently, the leading logarithmic contribution of the graph of Fig. (IV.1) to  $T_\mu^\mu$  is a factor of  $\ln\omega$  less than the ladder graph (with no crossed rungs) of order  $g^4$ . We have also calculated the leading logarithmic contribution of Fig. (IV.1) to  $T_2$  and find it also is factors of  $\ln\omega$  less than the ladder graph with uncrossed rungs of order  $g^4$ . We conjecture that all ladder graphs in the vector meson theory with crossed rungs in order  $g^{2N}$  have a leading logarithmic behavior which is at least a factor of  $\ln\omega$  less than that of the ladder graph with no crossed rungs of order  $g^{2N}$ . We have also examined the leading logarithm of the graph in Fig. (IV.1) in the neutral pseudo-scalar meson model and found it also had fewer logarithmic factors than the corresponding uncrossed ladder graph. This has also been shown by Chang and Fishbane.<sup>7</sup>

The graphs shown in Fig. (IV.2) also contribute to the forward virtual Compton amplitude. We have examined each of

these graphs in the neutral vector meson theory and the pseudo-scalar meson theory and found that each one's leading logarithmic behavior is at least a factor of  $\ln \omega$  less than the uncrossed ladder graph's leading behavior in the same order in  $g$ . Consequently, we conjecture that the leading logarithm comes from the ladder graphs (with uncrossed rungs) in each order of  $g$  in the neutral vector meson and neutral pseudoscalar meson theories. (This statement is also true in a charged pseudo-scalar meson theory.)

However there is a set of ladder graphs with uncrossed rungs which we have hitherto not considered. These graphs contain nucleon loops. They first appear in order  $g^4$  as shown in Fig. (IV.3).

We will show that the contribution of the diagram in Fig. (IV.3) to  $T_2$  has the same leading logarithmic behavior as the corresponding ladder graph without a nucleon loop in the neutral vector meson theory. We also show that the leading logarithm of the diagram in Fig. (IV.3) in the pseudoscalar meson theory has fewer logarithmic factors than the ladder diagram of order  $g^4$  without a nucleon loop. This is the only qualitative difference between the pseudoscalar meson theory and neutral vector meson theory calculations of the leading logarithmic behavior of the forward, virtual, Compton amplitude diagrams.

In evaluating the behavior of the diagram of Fig. (IV.3) with neutral vector mesons exchanged on the dashed lines we will use the same labeling of momenta and Feynman parameters as we did in Chapter II. Consequently we will have C and D

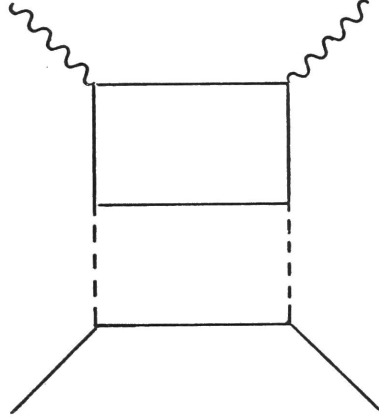


Fig. IV.3. Ladder Diagram With Nucleon Loop

given by eqs. (B4) and (B13) with  $N=2$ . The difference between this diagram's Feynman integral and that of the ladder diagram with two neutral vector meson rungs (which was studied in section III.B) occurs in  $\mathcal{N}_{2\mu\nu}$ . For this diagram  $\mathcal{N}_{2\mu\nu}$  is given by

$$\mathcal{N}_{2\mu} = \frac{-g^4}{4M} \text{Tr}[\not{p}\gamma^\lambda(\not{p}-\not{k}_2)\gamma^\sigma]\text{Tr}[\gamma_\lambda\not{k}_1\gamma_\mu(\not{A}+\not{k}_1)\gamma_\nu\not{k}_1\gamma_\sigma(\not{k}_2-\not{k}_1)] \quad (\text{IV.2})$$

where we have ignored masses since we are only interested in the leading behavior. We find that the leading logarithmic behavior comes from

$$\mathcal{N}_{2\mu\nu} \sim \frac{-8g^4}{M} k_1^2 k_2^2 [p_\mu (q+k_1)_\nu + (q+k_1)_\mu p_\nu - g_{\mu\nu} p \cdot (q+k_1)] \quad (\text{IV.3})$$

and leads to the following contributions to the  $p_\mu p_\nu$  and  $g_{\mu\nu}$  parts of  $W_{\mu\nu}$  :

$$\left( -g_{\mu\nu} + \frac{4p_\mu p_\nu}{|q^2|\omega^2} \right) \frac{\ln\omega}{2!M} \left( -\frac{g^2 \ln|q^2|}{8\pi^2} \right)^2 \quad (\text{IV.4})$$

A comparison of eq. (IV.3) with the evaluation of the  $P_n^b$  part of the trace in section III.B leads immediately to eq. (IV.4). The contribution of this diagram to the leading logarithmic behavior of  $W_1$  and  $W_2$  is exactly twice that of the order  $g^4$  ladder graph without nucleon loops studied in section III.B. It should be noted that the terms in  $\mathcal{N}_{2\mu\nu}$  in eq. (IV.2) which must be renormalized contribute to the Compton amplitude but not to its imaginary part.

We now consider the diagram in Fig. (IV.3) in the neutral pseudoscalar meson theory with dashed lines corresponding to pseudoscalar mesons. In this case the leading logarithmic behavior is at least a factor of  $\ln\omega$  less than the logarithmic behavior of the order  $g^4$  ladder diagram without a nucleon loop studied in section III.C. The diagram with crossed rungs and nucleon loops (Fig.(IV.4)) has fewer logarithmic factors than the order  $g^4$  ladder graph without nucleon loops in both the neutral vector meson and pseudoscalar meson theories.

We will now modify our neutral vector meson model so that it also included ladder diagrams containing nucleon loops.

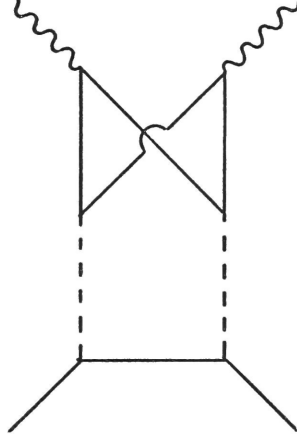


Fig. IV.4. A Nucleon Loop Diagram with Crossed Rungs.

First we note that the only possible diagrams with nucleon loops (and uncrossed rungs) in order  $g^6$  are given in Fig. (IV.5a) and (IV.5b). We find that the leading logarithmic term of each of these diagrams is exactly twice that of the diagram of Fig. (IV.5c) which was calculated in section III.B. In addition we found the numerical coefficient of

$$\prod_{i=1}^4 k_i^2 [p_\mu(q+k_1)_\nu + p_\nu(q+k_1)_\mu - g_{\mu\nu} p \cdot (q+k_1)]$$

in the traces from each of the diagrams of Fig. (IV.6). This part of the traces contains the leading logarithm. The

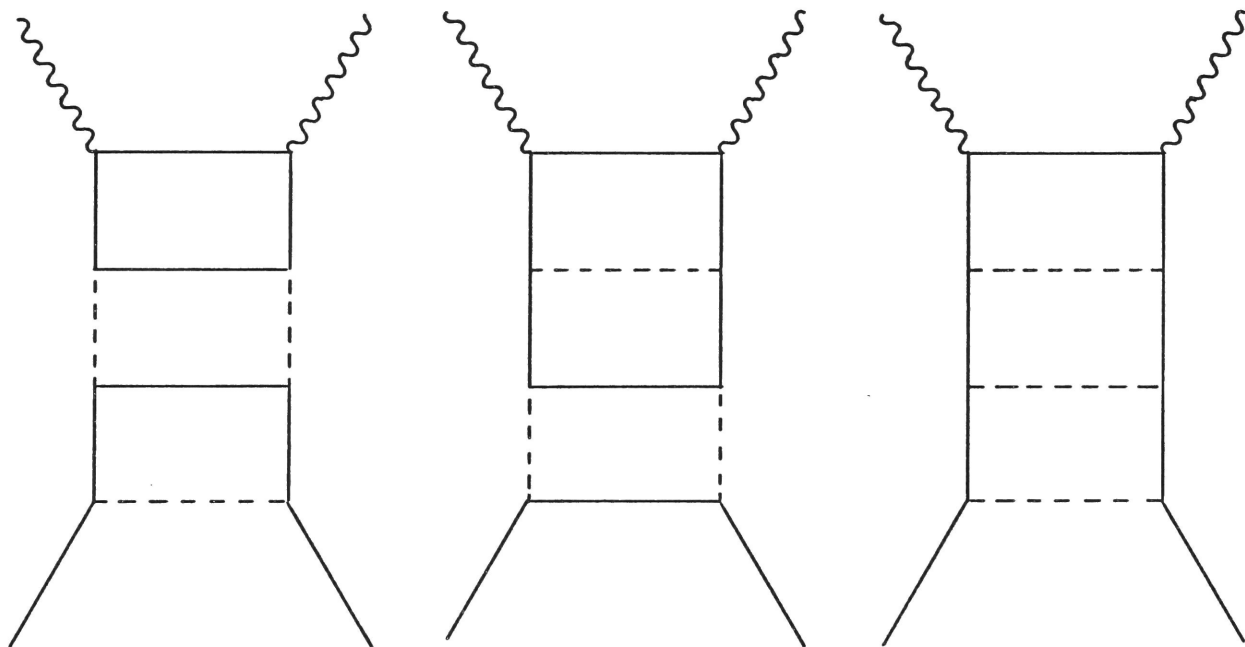


Fig. IV.5. The  $g^6$  Order Ladder Diagrams.

leading logarithm of diagram a of Fig. (IV.6) was calculated in section IIIb. The leading logarithm of diagrams b,c and d are each a factor of two greater than diagram a and the leading logarithm of diagram e is a factor of four greater than diagram a.

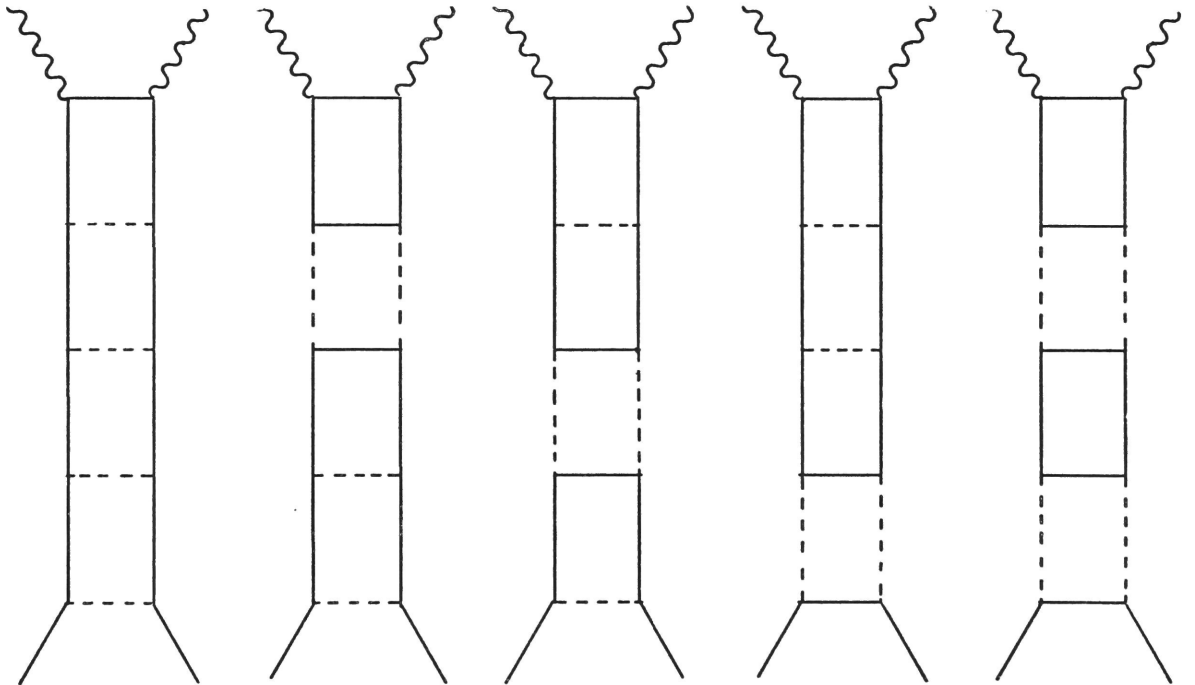


Fig. IV.6. The  $g^8$  Order Ladder Diagrams.

To make the combinatorics completely clear we give the ladder diagrams of order  $g^{10}$  and under each diagram write the numerical factor which gives the diagram's leading logarithm when multiplied times the leading logarithm of diagram (IV.7a) (previously calculated).

Consequently, the contribution of all  $(N+1)$  rung ladder diagrams in the neutral vector meson theory to the inelastic structure functions is a numerical multiple of the results given in eqs. (III.17) and (III.18) and the numeric factor is

$$f_N = \sum_{k=0}^{\left[\frac{N}{2}\right]} 2^k f_{Nk}$$

where  $f_{Nk}$  is the number of  $(N+1)$  rung ladder diagrams (with no crossed rungs) with  $k$  nucleon loops, and  $\left[\frac{N}{2}\right]$  is the greatest integer less than  $N/2$ . (The maximum number of nucleon loops in the  $N+1$  rung diagram is  $\left[\frac{N}{2}\right]$ .)

To compute  $f_{Nk}$  we note that (i) the number of nucleon loops in a ladder equals the number of pairs of neutral vector meson lines on the sides of the ladder, and (ii) no sub-diagrams of the form given in Fig. (IV.8) occur in any diagram. Furthermore, if we number the sides of each ladder graph with numbers as in Fig. (IV.9) then each ladder is in a one-to-one relationship with a set of numbers where the set consists of the numbers of sides which are dashed lines. Therefore, the number of ladders with  $N+1$  rungs and  $k$  nucleon loops,  $f_{Nk}$ , equals the number of different choices of  $k$  integers from the set  $\{1, 2, \dots, N-2\}$  such that no succession occurs in any choice. (A succession is a pair of numbers  $i$  and  $i+1$ , and is ruled



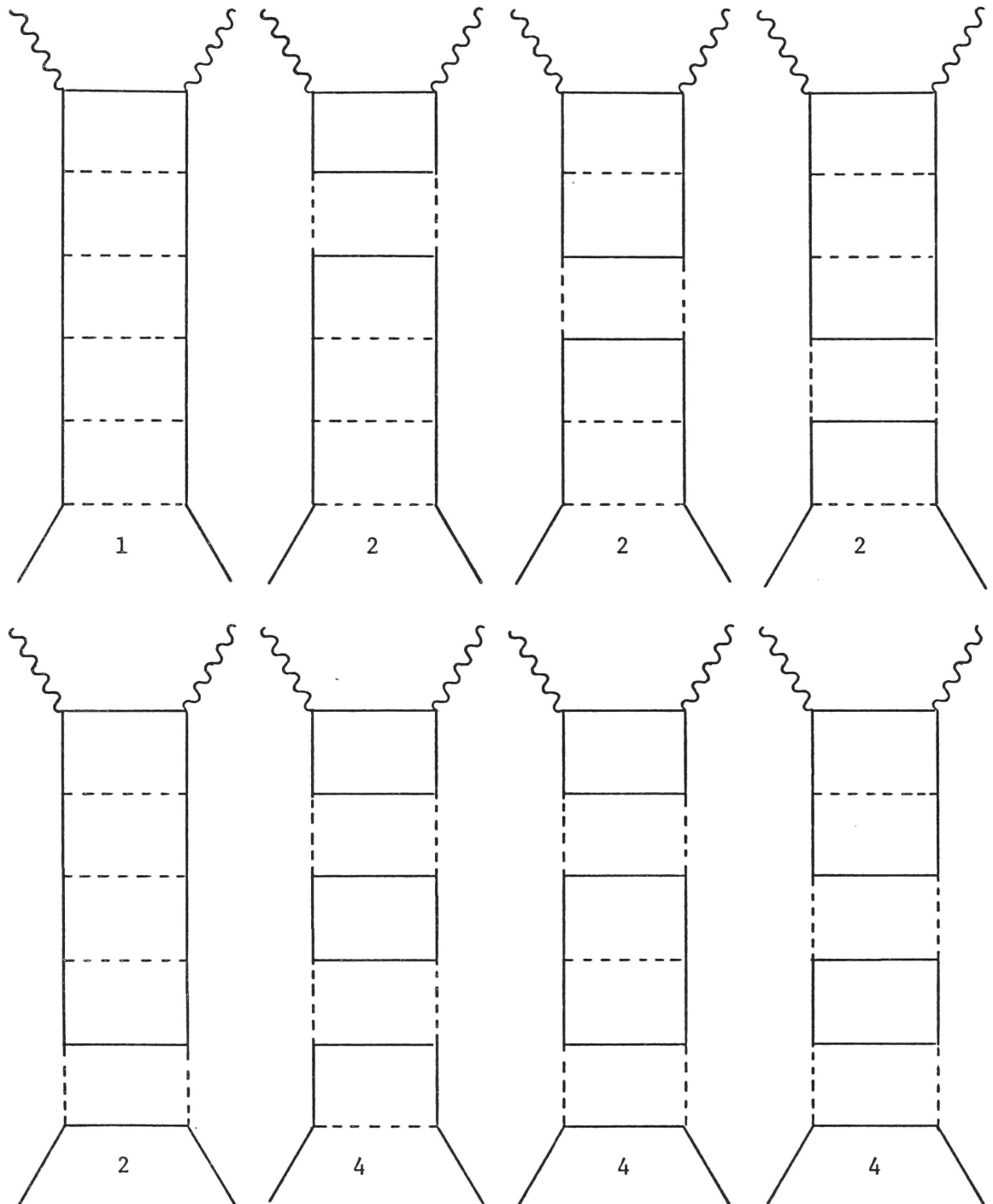


Fig. IV.7. The  $g^{10}$  Order Ladder Diagrams.

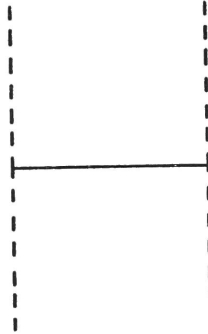


Fig. IV.8. A Sub-diagram Not Occurring in Field Theory.

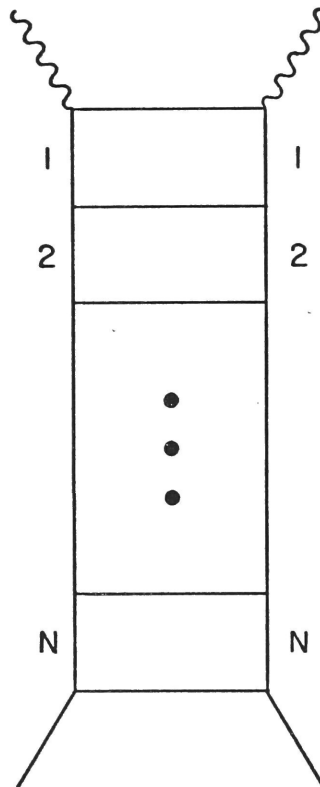


Fig.IV.9. Numbering of sides of ladders where solid lines represent neutral vector mesons or nucleons.

out by (ii).) This combinatorial relationship follows from rule (i) and the one-to-one relation of ladders and sets of numbers. The set  $\{1, 2, \dots, N-1\}$  is used rather than  $\{1, 2, \dots, N\}$  because side one is always a nucleon and there are thus only  $N-1$  possible locations for a neutral vector meson on the sides.

Riordan<sup>21</sup> gives an expression for  $f_{Nk}$  in its combinatorial context:

$$f_{Nk} = \binom{N-k}{k} \quad (\text{IV.5})$$

and also shows<sup>22</sup>

$$\begin{aligned} f_N &= \sum_{k=0}^{\lfloor \frac{N}{2} \rfloor} \binom{N-k}{k} 2^k \\ &= -\frac{1}{3} [2^{N+1} + (-1)^N] \end{aligned} \quad (\text{IV.6})$$

From eqs. (III.17), (III.18) and (IV.6) we find that the leading logarithm of the sum of all  $(N+1)$  rung ladder graphs in the neutral vector meson theory gives the following contribution to the structure functions:

$$\begin{aligned} W_{1N} &= \frac{[2^{N+1} + (-1)^N]}{6M^{1N}\omega N! (N-1)!} \left( \frac{g^2 \ln|q^2| \ln\omega}{8\pi^2} \right)^N \\ W_{2N} &= \frac{4M^2}{|q^2| \omega^2} W_{1N} . \end{aligned}$$

We sum over  $N$  and obtain

$$\begin{aligned} vW_2 &= \frac{g}{3\pi\omega} \left( \frac{\ln|q^2|}{\ln\omega} \right)^{\frac{1}{2}} I_1 \left( \frac{g}{\pi} \sqrt{\ln|q^2| \ln\omega} \right) - \\ &\quad - \frac{g}{6\sqrt{2}\pi\omega} \left( \frac{\ln|q^2|}{\ln\omega} \right)^{\frac{1}{2}} J_1 \left( \frac{g}{2\pi} \sqrt{\ln|q^2| \ln\omega} \right) \end{aligned} \quad (\text{IV.7})$$

$$MW_1 = \frac{\omega}{2} vW_2 \quad (\text{IV.8})$$

B. The Bethe-Salpeter Equations for the Neutral Vector Meson Model of the Virtual Compton Amplitude and its Relation to Jackiw's Bethe-Salpeter Equation for the Vertex.

The neutral vector meson madder model studied in chapter III is an iterative solution of the following Bethe-Salpeter equation:

$$T_{\mu\nu} = -\gamma_\mu \frac{1}{\not{p} + \not{q} - M} \gamma_\nu - \frac{ig^2}{(2\pi)^4} \int \frac{d^4k \gamma_\alpha (\not{k} + M) \gamma_{\mu\nu} (\not{k} + M) \gamma^\alpha}{[(p-k)^2 - m^2][k^2 - M^2]^2} \quad (\text{IV.9})$$

The diagrammatic representation of this equation is given in Fig. (IV.10).

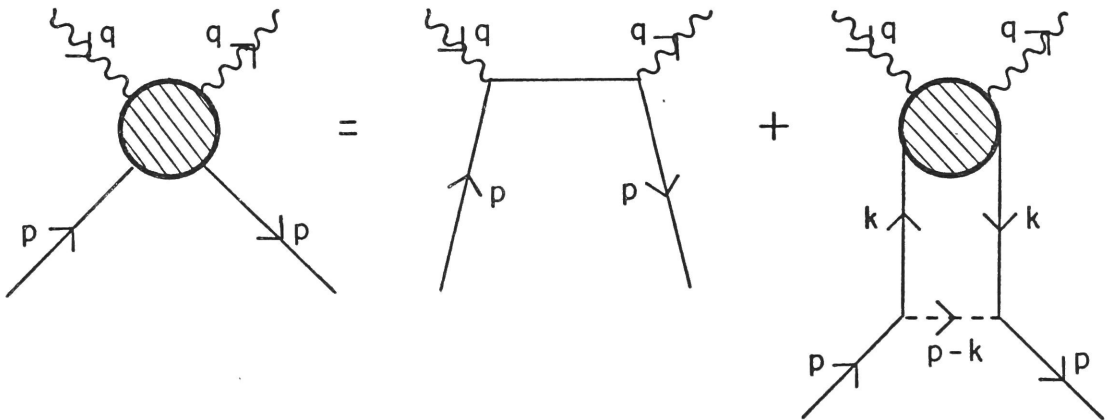


Fig. IV.10. Diagram Corresponding To a Bethe-Salpeter Equation

If we put the nucleon on the mass shell and spin average we obtain the forward virtual Compton amplitude

$$T_{\mu\nu} = \frac{1}{4M} \text{Tr}(\not{p} + M) \mathcal{T}_{\mu\nu} \quad (\text{IV.10})$$

We will now investigate the asymptotic behavior of eq. (IV.9) when  $|q^2| \rightarrow \infty$  and  $\omega$  is large and fixed. After finding an approximate integral equation which contains the leading logarithmic behavior (previously studied) we relate it to the integral equation of Jackiw<sup>20</sup> for the electromagnetic vertex.

For reasons of simplicity which will be apparent later we will restrict ourselves to a consideration of  $\mathcal{T}_{\mu}^{\mu} = \mathcal{T}$  which corresponds to  $-3T_1 + \frac{\omega}{2M} vT_2$  in the limit  $|q^2| \rightarrow \infty$  with  $\omega = 2q \cdot p / |q^2|$  fixed. From our study of the spinor factors of the iterations of eq. (IV.9) in Appendix A it is clear that  $\mathcal{T}$  may be written

$$\mathcal{T} = \mathcal{T}_1 + \not{x} \mathcal{T}_2 + \not{A} \mathcal{T}_3 \quad (\text{IV.11})$$

(We are not interested in solutions of the homogeneous integral equation.) Consequently, we obtain

$$\gamma_{\alpha}(\not{k} + M) \mathcal{T}(\not{k} + M) \gamma^{\alpha} = 2(k^2 - M^2)(\not{A} \mathcal{T}_3 - \not{k} \mathcal{T}_2) + \dots \quad (\text{IV.12})$$

where we have made only the part giving the leading logarithmic behavior explicit on the right side of the equation. We know the leading part from our calculations in Chapter III. Since we are only interested in the leading behavior we will drop the other terms. The result is the integral equation

$$\mathcal{T}_1 + \not{p} \mathcal{T}_2 + \not{q} \mathcal{T}_3 = \frac{2(\not{p} + \not{q} - 2M)}{(p+q)^2 - M^2} - \frac{2ig^2}{(2\pi)^4} \int \frac{d^4k (-\not{k} \mathcal{T}_2 + \not{q} \mathcal{T}_3)}{[(p-k)^2 - m^2][k^2 - M^2]} \quad (\text{IV.13})$$

By taking traces of the above equation it is clear

$$\mathcal{T}_1 = -4M[p+q]^2 - M^2] \quad (\text{IV.14})$$

$$p^2 \mathcal{T}_2 + p \cdot q \mathcal{T}_3 = \frac{2(p^2 + p \cdot q)}{(p+q)^2 - M^2} - \frac{2ig^2}{(2\pi)^4} \int \frac{d^4k (-p \cdot k \mathcal{T}_2 + q \cdot p \mathcal{T}_3)}{[(p-k)^2 - m^2][k^2 - M^2]} \quad (\text{IV.15})$$

$$p \cdot q \mathcal{T}_2 + q^2 \mathcal{T}_3 = \frac{2(p \cdot q + q^2)}{(p+q)^2 - M^2} - \frac{2ig^2}{(2\pi)^4} \int \frac{d^4k (-q \cdot k \mathcal{T}_2 + p \cdot q \mathcal{T}_3)}{[(p-k)^2 - m^2][k^2 - M^2]} \quad (\text{IV.16})$$

An equation for  $\mathcal{T}_2$  can be obtained by taking the difference of  $q^2$  times the second equation and  $p \cdot q$  times the third equation:

$$\mathcal{T}_2 = \frac{2}{(p+q)^2 - M^2} - \frac{2ig^2}{(2\pi)^4 [q^2 p^2 - (p \cdot q)^2]} \int \frac{d^4k (q \cdot p q \cdot k - q^2 p \cdot k) \mathcal{T}_2}{[(p-k)^2 - m^2][k^2 - M^2]} \quad (\text{IV.17})$$

We find that the leading logarithmic behavior of the iterations of this equation in the limit  $|q^2| \rightarrow \infty$  with  $\omega$  large and fixed are  $\frac{1}{\omega}$  less than the corresponding behavior of  $\mathcal{T}_3$ . As a result we obtain a good approximation to the leading behavior of  $\mathcal{T}_3$  if we set  $\mathcal{T}_2 = 0$  in eq. (IV.15). This equation becomes

$$\mathcal{T}_3 = \frac{2}{(p+q)^2 - M^2} - \frac{2ig^2}{(2\pi)^4} \int \frac{d^4k \mathcal{T}_3}{[(p-k)^2 - m^2][k^2 - M^2]} \quad (\text{IV.18})$$

upon neglecting  $p^2$  with respect to  $p \cdot q$  in the Born term.

Next we let

$$S = \frac{1}{2} [(p+q)^2 - M^2] \mathcal{T}_3 \quad (\text{IV.19})$$

which transforms eq. (IV.18) into

$$S = 1 - \frac{2ig^2}{(2\pi)^4} [(q+p)^2 - M^2] \int \frac{d^4k S}{[(p-k)^2 - m^2][k^2 - M^2][(q+k)^2 - M^2]} \quad (\text{IV.20})$$

Before relating eq. (IV.20) to Jackiw's equation for the electromagnetic vertex we will find the leading logarithmic behavior of  $S$  in the limit  $|q^2| \rightarrow \infty$  with  $\omega$  large and fixed from our calculations of section III.B. From eq. (I.14) we obtain

$$T_\mu^\mu = -3T_1 + \frac{\omega}{2M} \nu T_2 \quad (\text{IV.21})$$

The asymptotic behavior of the  $(N+1)$  rung diagram which is given in eqs. (III.7) and (III.9) implies

$$T_\mu^\mu \cong \frac{1}{M} I_0 \left( \frac{g}{2\pi} \sqrt{2 \ln |q^2| \ln \omega} \right) \quad (\text{IV.22})$$

upon summation over  $N$  and insertion of the results in eq. (IV.21). From eqs. (IV.10), (IV.11) and (IV.19) we obtain

$$\begin{aligned} T_\mu^\mu &= \frac{1}{4M} \text{Tr } \not{p} \not{q} \not{p} \not{q} \\ &= \frac{2 p \cdot q}{M[(p+q)^2 - M^2]} S \\ &= \frac{1}{M} S \end{aligned} \quad (\text{IV.23})$$

or

$$S \cong I_0 \left( \frac{g}{2\pi} \sqrt{2 \ln |q^2| \ln \omega} \right) \quad (\text{IV.24})$$

as  $|q^2| \rightarrow \infty$  with  $\omega$  large and fixed. Eq. (IV.24) can be verified

by finding the leading logarithmic behavior of the iterations of eq. (IV.20).

Next we examine Jackiw's integral equation for the nucleon electromagnetic vertex in a neutral vector meson ladder model. The equation for the vertex function,  $\Gamma$ , given in eq. (IV.17) of Jackiw is

$$\Gamma = 1 + \frac{2ig^2q^2}{(2\pi)^4} \int \frac{d^4k\Gamma}{[(p-k)^2-m^2][k^2-M^2][(q+k)^2-M^2]} \quad (\text{IV.25})$$

in our notation. A diagrammatic representation of this equation is given in Fig. (IV.11).

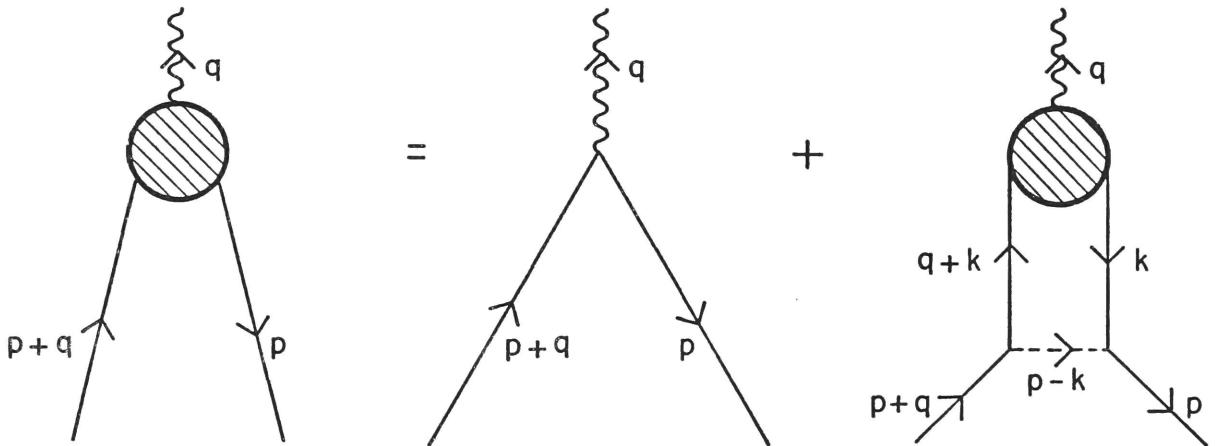


Fig. IV.11. Diagram Corresponding To Vertex Integral Equation.



Jackiw's off-mass-shell solution of eq. (IV.25) in the asymptotic region

$$\frac{|(q+p)^2||p^2|}{m^2} \gg |q^2| \gg |(q+p)^2|, |p^2| \gg M^2 \quad (\text{IV.26})$$

is

$$\Gamma = J_0 \left( \frac{g}{2\pi} \sqrt{2 \ln \left| \frac{q^2}{p^2} \right| \ln \left| \frac{q^2}{(p+q)^2} \right|} \right) \quad (\text{IV.27})$$

The similarity of the integral equations (eq. (IV.20) and eq. (IV.25)) is obvious. If we remember that the solution for  $S$  was in the region where  $(q+p)^2 \approx 2q \cdot p$  then we find that  $S$  and  $\Gamma$  are identical (eqs. (IV.24) and (IV.27)). Thus the asymptotic behavior of the virtual Compton amplitude is the same as the asymptotic behavior of the off-mass-shell vertex function in the neutral vector meson ladder model. It should be noted that the asymptotic regions are not the same.

### C. Comparison With Experiment

We will make a qualitative comparison of the structure functions which we have found with the experimental data. As we pointed out in Chapter I the outstanding qualitative feature of the data was the scaling of  $\nu W_2$ . Therefore an examination of Table (IV.1) shows that the models of cases 1 and 4 do not agree with the experiment. The other models may agree with experiment. The model of case I is essentially unphysical and will be disregarded. The neutral vector meson and neutral pseudoscalar meson models (case 4) can have their disagreement with experiment explained in two ways: (i) they are fundamentally inconsistent with physical reality or (ii) the effect of non-leading logarithms is

significant and must be included to obtain a realistic model.

The models in which scaling does occur either have a "scalar" nucleon which is unphysical, or introduce a cutoff in the transverse momentum of pions emitted at pion-nucleon vertices (case 5). The introduction of a momentum cutoff by Drell, Levy and Yan<sup>11</sup> is based on the observed distribution of pion momenta in various experiments. Their results, eqs. (I.19), agree with the experimental data with the "correct" choice of values for the parameters.

The inelastic structure functions are related to the longitudinal cross-section,  $\sigma_L$ , and the transverse cross-section,  $\sigma_T$ , by<sup>23</sup>

$$W_1 = \left(1 + \frac{v^2}{|q^2|}\right) \frac{\sigma_T}{\sigma_T + \sigma_L} W_2$$

$$\approx \frac{v^2}{|q^2|} \frac{\sigma_T}{\sigma_T + \sigma_L} W_2$$
(IV.28)

in the limit  $|q^2| \rightarrow \infty$  with  $\omega$  fixed. Since all the spin  $\frac{1}{2}$  nucleon model structure functions satisfy eq. (I.19b) we have  $\sigma_L = 0$ . Experimentally<sup>1</sup>  $\sigma_L/\sigma_T$  is quite small with an average value of .18. Since we only kept leading logarithms the difference between our results and experiment is not surprising.

After our work was completed we learned that Chang and Fishbane<sup>7</sup> had also calculated  $W_2$  in a neutral pseudoscalar meson model. They used infinite momentum frame techniques and obtained a result which agrees with ours. More recently Gaisser and Polkinghorne,<sup>24</sup> and Choudhury and Varma<sup>25</sup> have

Table IV.1

Ladder Model	non-scaling $ q^2 $ behavior of the (N+1) rung ladder contribution to	
	$W_1$	$W_2$
1. All particles spinless		1
2. Spin 1 photons. All other particles are mesons in a $\phi^3$ theory.	$\frac{\ln  q^2 }{ q^2 }$	1
3. Spin 1 photons. All other particles are mesons in a truss bridge diagram theory.	$\frac{(\ln  q^2 )^N}{ q^2 }$	1
4. Spin 1 photons, spin $\frac{1}{2}$ nucleons, neutral vector mesons <u>or</u> pseudoscalar mesons on the ladder's rungs.	$(\ln  q^2 )^N$	$(\ln  q^2 )^N$
5. Model 4. with a transverse momentum cutoff at pion-nucleon vertices.	1	1

studied spin one-half nucleon ladder models and obtained similar results.

#### D. Neutrino-Nucleon Scattering

In this section we study a neutral vector meson and neutral pseudoscalar meson model of neutrino-nucleon scattering. Our procedure is based on the calculations of sections III.B and III.C.

If we define our kinematic variables as in section I.B then the inelastic cross-section for the scattering of a neutrino,  $\nu$ , (or an anti-neutrino,  $\bar{\nu}$ ) off an unpolarized nucleon can be written (we ignore terms proportional to lepton masses)

$$\frac{d\sigma(\frac{\nu}{\bar{\nu}})}{d\Omega dE'} = \frac{E'^2 G^2}{2\pi^2} \left[ \cos^2\left(\frac{\theta}{2}\right) W_2(\frac{\nu}{\bar{\nu}}) + 2 \sin^2\left(\frac{\theta}{2}\right) W_1(\frac{\nu}{\bar{\nu}}) + \frac{E+E'}{M} \sin^2\left(\frac{\theta}{2}\right) W_3(\frac{\nu}{\bar{\nu}}) \right] \quad (\text{IV.29})$$

with

$$W_{\mu\nu}(\frac{\nu}{\bar{\nu}}) = \frac{1}{2\pi} \int d^4x e^{iq \cdot x} \langle p | [J_\mu^\dagger(x), J_\nu(0)] | p \rangle \quad (\text{IV.30})$$

$$\begin{aligned} &= -(g_{\mu\nu} - \frac{q_\mu q_\nu}{q^2}) W_1(\frac{\nu}{\bar{\nu}}) + \frac{1}{M^2} (p_\mu - \frac{p \cdot q}{q^2} q_\mu) (p_\nu - \frac{p \cdot q}{q^2} q_\nu) W_2(\frac{\nu}{\bar{\nu}}) - \\ &- i\epsilon_{\mu\nu\alpha\beta} \frac{q^\alpha q^\beta}{2M} W_3(\frac{\nu}{\bar{\nu}}) \end{aligned} \quad (\text{IV.31})$$

The normalization is such that the bare weak current evaluated between a point-like proton state of momentum  $p$  and neutron state of momentum  $p_n$  is given by

$$\langle p | J_\mu^+ | p_n \rangle = -i \bar{u}(p) \gamma_\mu (1 - \gamma_5) u(p_n)$$

(We have set the Cabibbo angle equal to zero and  $g_A = g_V$ .)

Our model has the weak current attached where the photon had been attached in the models of Chapter III. Fig. (IV.12) gives the (N+1) rung ladder diagram. Obviously we can use our previous calculations to find the structure functions. We need only insert factors of  $(1-\gamma_5)$  in the appropriate places in the traces previously considered in sections III.B and III.C. Thus

$$\mathcal{N}_{N\mu\nu} = \frac{-g^2}{4M} \text{Tr}[\gamma_\mu (1-\gamma_5) (\not{q} + \not{k}_1 + M) \gamma_\nu (1-\gamma_5) P_N] \quad (\text{IV.32})$$

is the appropriate numerator expression for neutrino scattering in both the pseudoscalar and neutral vector meson results. From our expression for  $P_N$  given in eq. (A1) and our calculations in sections III.B and III.C we find that the leading logarithmic behavior of the structure functions comes from the following part of  $\mathcal{N}_{N\mu\nu}$

$$\begin{aligned} & \frac{-2g^2 P_N^b}{M} [(q+k_1)_\mu p_\nu + (q+k_1)_\nu p_\mu - p \cdot (q+k_1) g_{\mu\nu} + \\ & + i\epsilon_{\mu\nu\alpha\beta} p^\alpha (q+k_1)^\beta] \end{aligned} \quad (\text{IV.33})$$

Comparing eq. (IV.33) with the analogous expressions in Chapter III we find

$$W_1^{(\frac{\nu}{\nu})} = 2 W_{1EM} \quad (\text{IV.34a})$$

$$W_2^{(\frac{\nu}{\nu})} = 2 W_{2EM} \quad (\text{IV.34b})$$

$$W_3^{(\frac{\nu}{\nu})} = \frac{-4M^2}{q \cdot p} W_{1EM} \quad (\text{IV.34c})$$

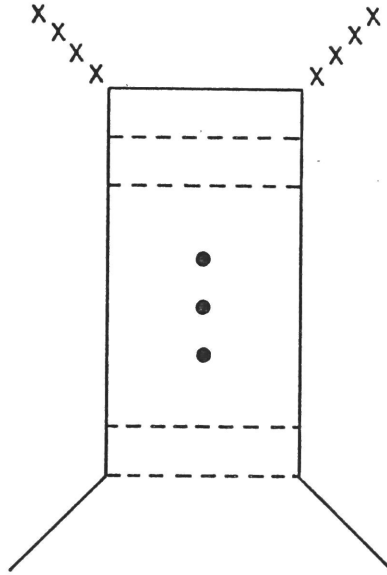


Fig. IV.12. The Ladder Diagram Relevant to Neutrino-Nucleon Scattering.

where  $W_1^\nu$  is for  $\nu$ -neutron scattering and  $W_1^{\bar{\nu}}$  is for  $\bar{\nu}$ -proton scattering and where the relation between the neutrino structure functions on the left and the electron-nucleon structure functions on the right holds in both the neutral pseudoscalar meson ladder model and the neutral vector meson ladder model. Eq. (IV.34c) follows quickly from a comparison of the coefficients of  $g_{\mu\nu}$

and  $\epsilon_{\mu\nu\alpha\beta}$  in eqs. (IV.31) and (IV.33). From eqs. (IV.34) we obtain

$$MW_1^{(\nu)} = \frac{\omega}{2} \nu W_2^{(\nu)} = -\frac{1}{2} \nu W_3^{(\nu)} \quad (\text{IV.35})$$

which agrees with the relations found by Drell, Levy and Yan<sup>26</sup> in their model.

### Appendix A. The Spinor Polynomial

The spinor polynomial,

$$P_N = (\not{k}_1 + M) \gamma^{\alpha_1} (\not{k}_2 + M) \gamma^{\alpha_2} \dots (\not{k}_N + M) \gamma^{\alpha_N} (\not{p} + M) \gamma_{\alpha_N} (\not{k}_N + M) \dots \gamma_{\alpha_{N-1}} \dots (\not{k}_2 + M) \gamma_{\alpha_1} (\not{k}_1 + M) \quad (A1)$$

can be calculated from a set of recurrence relations. If we let  $L_{N+1-i} = k_i$  then

$$P_N = (\not{L}_N + M) \gamma^\alpha P_{N-1} \gamma_\alpha (\not{L}_N + M) \quad (A2)$$

with  $P_0 = \not{p} + M$ . A simple induction in which the form of  $P_0$  and the recurrence relations to be derived play the key roles proves that we may write

$$P_N = P_N^a + \not{p} P_N^b + \sum_{i=1}^N P_N^i \not{L}_i \quad (A3)$$

with  $P_N^j$  being a scalar function of inner products of the momenta.

Using eq. (A3) on both sides of eq. (A2) and the Dirac algebra of the  $\gamma$ -matrices we obtain the following recurrence relations

$$P_N^a = 4 (L_N^2 + M^2) P_{N-1}^a - 4M \not{p} \cdot L_N P_{N-1}^b - 4M \sum_{j=1}^{N-1} P_N^j L_j \cdot L_N \quad (A4)$$

$$P_N^b = 2 (L_N^2 - M^2) P_{N-1}^b \quad (A5)$$

$$P_N^j = 2 (L_N^2 - M^2) P_{N-1}^j \quad j = 1, 2, \dots, N-1 \quad (A6)$$



$$P_N^N = 8M P_{N-1}^a - 4 P \cdot L_N P_{N-1}^b - 4 \sum_{j=1}^{N-1} P_{N-1}^j L_j \cdot L_N \quad (A7)$$

We now solve this set of recurrence relations. Eq. (A5) implies

$$P_N^b = 2^N \prod_{i=1}^N (L_i^2 - M^2) \quad (A8)$$

and similarly eq. (A6) implies

$$P_N^j = 2^{N-j} P_j^j \prod_{i=j+1}^N (L_i^2 - M^2) \quad (A9)$$

for  $j = 1, 2, \dots, N-1$ . In addition, eqns. (A4) and (A7) lead to

$$P_N^a - M P_N^N = 4(L_N^2 - M^2) P_{N-1}^a \quad (A10)$$

We now iterate eq. (A10) which results in

$$P_N^a = M \sum_{j=0}^N 4^{N-j} P_j^j \prod_{i=j+1}^N (L_i^2 - M^2) \quad (A11)$$

with  $P_0^0 = 1$ . The use of eqns. (A11), (A8) and (A9) in eq. (A7) enables us to put  $P_N^N$  in the following form:

$$P_N^N = \sum_{j=0}^{N-1} A_j^N P_j^j \quad (A12)$$

where

$$A_i^j = 2 (M^2 4^{j-i} - L_j \cdot L_i 2^{j-i}) \prod_{r=i+1}^{j-1} (L_r^2 - M^2) \quad (A13)$$

Eq. (A12) leads directly to the solution for  $P_N^N$ :

$$P_N^N = \sum_{s=0}^{N-1} \sum_{1 \leq i_1 < i_2 < \dots < i_s < N} A_0^{i_1} A_{i_1}^{i_2} A_{i_2}^{i_3} \dots A_{i_{s-1}}^{i_s} A_{i_s}^N \quad (A14)$$

with the  $s = 0$  term being  $A_0^N$  and with  $L_0 = p$ . We have now solved the recurrence relations since eq. (A14) can be used in Eqns. (A9) and (A11), respectively, in order to give

$$P_N^j = 2^{N-j} \prod_{i=j+1}^N (L_i^2 - M^2) \sum_{s=0}^{j-1} \sum_{1 \leq i_1 < \dots < i_s < j} A_0^{i_1} A_{i_1}^{i_2} \dots A_{i_s}^j \quad (\text{A15})$$

and

$$P_N^a = M \sum_{j=0}^{N-1} 2^{N-j} \prod_{i=j+1}^N (L_i^2 - M^2) \sum_{s=0}^{j-1} \sum_{1 \leq i_1 < \dots < i_s < j} A_0^{i_1} A_{i_1}^{i_2} \dots A_{i_s}^j \quad (\text{A16})$$

$$= M \sum_{j=0}^N 2^{N-j} P_N^j. \quad (\text{A17})$$

We now express (A8) and (A15) in terms of the loop momenta,  $k_i = L_{N+1-i}$ :

$$P_N^b = 2^N \prod_{i=1}^N (k_i^2 - M^2) \quad (\text{A18})$$

and

$$\begin{aligned} P_N^i = P_N^{N+1-i} &= 2^{i-1} \prod_{r=1}^{i-1} (k_r^2 - M^2) \sum_{s=0}^{N-i} \sum_{1 \leq a_1 < a_2 < \dots < a_s \leq N} B_{i_1}^{a_1} \dots B_{a_1}^{a_2} \dots B_{a_{s-1}}^{a_s} B_{a_s}^{N+1} \\ &\quad \cdot B_{a_1}^{a_2} \dots B_{a_{s-1}}^{a_s} B_{a_s}^{N+1} \end{aligned} \quad (\text{A19})$$

with

$$B_b^a = 2(4^{a-b} M^{2-2^{a-b}} k_a \cdot k_b) \prod_{r=b+1}^{a-1} (k_r^2 - M^2) \quad (\text{A20})$$

and the conventions  $k_{N+1} = p$ ,  $P_N^{N+1} = 1$ , and  $\prod_{r=a+1}^a (k_r^2 - M^2) = 1$  whenever it occurs. The reason for having the superscript  $N+1-i$  on  $P_N^j$  in eq. (A19) becomes clear when we rewrite eq. (A3)

$$\begin{aligned}
P_N &= P_N^a + \not{A} P_N^b + \sum_{i=1}^N P_N^{N+1-i} \not{\epsilon}_i \\
&= P_N^a + \not{A} P_N^b + \sum_{i=1}^N \tilde{P}_N^i \not{\epsilon}_i
\end{aligned} \tag{A21}$$

The spinor polynomial for the  $\gamma_5$  meson-nucleon case can be calculated in a similar fashion. Let  $P_N^a$ ,  $P_N^b$  and  $P_N^i$  be defined as in eq. (A3). Then using

$$P_N = (\not{L}_N + M) \gamma_5 P_{N-1} \gamma_5 (\not{L}_N + M) \tag{A22}$$

we obtain the following recurrence relations:

$$P_N^a = (L_N^2 + M^2) P_{N-1}^a - 2 M P_N \cdot L_N P_{N-1}^b - 2 M \sum_{j=1}^{N-1} P_{N-1}^j L_j \cdot L_N \tag{A23}$$

$$P_N^b = (L_N^2 - M^2) P_{N-1}^b \tag{A24}$$

$$P_N^i = (L_N^2 - M^2) P_{N-1}^i \quad i = 1, 2, \dots, N-1 \tag{A25}$$

$$P_N^N = 2 M P_{N-1}^a - 2 P_N \cdot L_N P_{N-1}^b - 2 \sum_{j=1}^{N-1} P_{N-1}^j L_j \cdot L_N . \tag{A26}$$

If we proceed in exactly the same fashion as the previous case we obtain

$$P_N^b = \prod_{i=1}^N (k_i^2 - M^2) \tag{A27}$$

$$P_N^a = M \sum_{j=0}^N \tilde{P}_N^{N+1-j} \tag{A28}$$

$$\tilde{P}_N^j = \prod_{r=1}^{j-1} (k_r^2 - M^2) \sum_{s=0}^{N-j} \sum_{j < a_1 < \dots < a_s \leq N} E_j^{a_1} E_{a_1}^{a_2} \dots E_{a_s}^{N+1} \tag{A29}$$

with

$$E_i^j = 2(M - k_i \cdot k_j) \prod_{r=i+1}^{j-1} (k_r^2 - M^2). \quad (\text{A30})$$

and the conventions  $\tilde{P}_N^{N+1} = 1$ ,  $k_{N+1} = p$  and  $\prod_{r=k+1}^k (k_r^2 - M^2)$  is taken to be 1 wherever it might appear.

158845

## Appendix B. The Feynman Parameter Polynomials C and D

Given a Feynman diagram whose internal lines have been labelled with Feynman parameters there are two unique polynomials, usually denoted C and D, which are determined by the geometry of the diagram. C is a homogeneous polynomial in the Feynman parameters, and D is a homogeneous polynomial in the Feynman parameters and scalar products of the diagrams' external momenta. If the diagram has N independent loop momenta associated with it then C is of degree N and D of degree N+1 in the Feynman parameters.

In order to determine C for a graph we follow a procedure given by Eden et al.<sup>13</sup> First determine all sets of lines such that each set satisfies the following conditions. If we "cut" every line of the set in the Feynman diagram then (i) every vertex in the diagram is connected to every other vertex by a sequence of uncut lines and (ii) no further lines may be cut without violating (i). To each set of lines satisfying these conditions corresponds a term in C consisting of the product of the Feynman parameters of the lines in the set. C is the sum of all such terms.

The determination of D is slightly different from that of C. It may be written,  $D = \chi - \sigma C$  where  $\sigma$  is the sum over all internal lines in the graph of the squared mass of the particle associated with a line times the Feynman parameter of the line. In order to find  $\chi$  we first determine all sets of lines such that cutting lines of a given set in the Feynman diagram divides the graph into two disjoint parts (there is no sequence of uncut lines going from one part to the other) and such that

rules (i) and (ii) above hold in each part. To each such set there is a term in  $\chi$  consisting of the product of the Feynman parameters of the lines in the set times the squared sum of all external momenta entering into either of the disjoint parts.

We now turn to a consideration of the (N+1) rung ladder diagram of Fig. (II.2).

We define  $C_j^i = C_j^i(\alpha_i, \alpha_{i+1}, \dots, \alpha_j, \beta_{i+1}, \beta_{i+2}, \dots, \beta_j, \gamma_{i+1}, \gamma_{i+2}, \dots, \gamma_j)$  to be the homogeneous polynomial (of order  $j-i$ , in the Feynman parameters) which is associated with the graph obtained (Fig. (II.2)) by deleting all lines above the rung labelled with  $\alpha_i$  and below the rung labelled with  $\alpha_j$ . Thus the polynomial,  $C$ , associated with the entire graph in (Fig. (II.2)) would be denoted  $C_N^0$ . If we let

$$d_{ij} = \alpha_i \alpha_{i+1} \dots \alpha_j \quad (B1)$$

for  $i \leq j$  then the recurrence relations for the  $C_j^i$  are given by

$$C_j^i = d_{i+1,j}^{+(\alpha_i + \beta_{i+1} + \gamma_{i+1})} C_j^{i+1} + \sum_{k=i+1}^{j-1} d_{i+1,k}^{(\beta_{k+1} + \gamma_{k+1})} C_j^{k+1} \quad (B2)$$

$$C_j^i = d_{i,j-1}^{+(\alpha_j + \beta_j + \gamma_j)} C_{j-1}^i + \sum_{k=i+1}^{j-1} d_{k,j-1}^{(\beta_k + \gamma_k)} C_{k-1}^i \quad (B3)$$

with  $C_k^k = 1$ . In particular,

$$C_N^0 = d_{1N}^{+(\alpha_0 + \beta_1 + \gamma_1)} C_N^1 + \alpha_1 (\beta_2 + \gamma_2) C_N^2 + \dots + d_{1,N-1}^{(\beta_N + \gamma_N)} \quad (B4)$$

$$= d_{0,N-1}^{+(\alpha_N + \beta_N + \gamma_N)} C_{N-1}^0 + \alpha_{N-1} (\beta_{N-1} + \gamma_{N-1}) C_{N-2}^0 + \dots + d_{1,N-1}^{(\beta_1 + \gamma_1)}. \quad (B5)$$

The homogeneous polynomial,  $D$ , of order,  $N+1$ , in the Feynman parameters and containing scalar products of the external momenta in Fig. (III.2) has the form

$$D = G(q+p+A_0)^2 + \sum_{i=1}^N [(q+A_0-A_i)^2 G_i + (p+A_i)^2 H_i] + \sum_{\substack{i,j=1 \\ i < j}}^N (A_i - A_j)^2 I_{ij} - \alpha_0 M^2 C - \sum_{i=1}^N [M^2(\beta_i + \gamma_i) + m^2 \alpha_i] C \quad (B6)$$

with  $G$ ,  $G_i$ ,  $H_i$  and  $I_{ij}$  functions of Feynman parameters only. We now give the explicit form of these functions which follow immediately from rules given in reference 13.

$$G = d_{0N} \quad (B7)$$

$$G_i = d_{0,i-1}(\beta_i + \gamma_i) C_N^i \quad (B8)$$

$$H_i = d_{iN}(\beta_i + \gamma_i) C_{i-1}^0 \quad (B9)$$

$$I_{ij} = d_{i,j-1}(\beta_i + \gamma_i)(\beta_j + \gamma_j) C_{i-1}^0 C_N^j \quad (B10)$$

If we note that eqns. (B4) and (B5) imply

$$G + \sum_{i=1}^N G_i = \alpha_0 (C - \alpha_0 C_N^1) \quad (B11)$$

$$G + \sum_{i=1}^N H_i = \alpha_N (C - \alpha_N C_{N-1}^0) \quad (B12)$$

then

$$D(0) = D \left| A_0 = A_1 = \dots = A_N = 0 = \alpha_0 q^2 (\rho d_{1N} + C') + \alpha_N M^2 (C - \alpha_N C_{N-1}^0) - \alpha_0 M^2 C - \right. \\ \left. - C \sum_{i=1}^N [M^2 (\beta_i + \gamma_i) + m^2 \alpha_i] = \alpha_0 q^2 (\rho d_{1N} + C') + JC \right. \quad (B13)$$

$$\text{with } \rho = \frac{2q \cdot p}{q^2} \text{ and } C' = C - \alpha_0 C_N^1 = C \Big|_{\alpha_0 = 0}.$$

We now calculate

$$I_j = \sum_{k < j} I_{kj} + \sum_{k < j} I_{jk}.$$

from eqns. (B2) , (B3) and (B10) for later use in Appendix C:

$$I_j = (\beta_j + \gamma_j) \left[ C_N^j \sum_{k=1}^{j-1} d_{k,j-1} (\beta_k + \gamma_k) C_{k-1}^0 + C_{j-1}^0 \sum_{k=j+1}^N d_{j,k-1} (\beta_k + \gamma_k) C_N^k \right] \\ = (\beta_j + \gamma_j) \left[ \alpha_{j-1} C_N^j (C_{j-1}^0 - d_{0,j-2} - \alpha_{j-1} C_N^{j+1}) + \alpha_j C_{j-1}^0 (C_N^j - d_{j+1,N} - C_N^{j+1} \alpha_j) \right] \quad (B14)$$

for  $j = 2, 3, \dots, (N-1)$ . For  $j = 1$  and  $j = N$   $I_j$  has the following form:

$$I_1 = (\beta_1 + \gamma_1) \alpha_1 (C_N^1 - d_{2N} - \alpha_1 C_N^2) \quad (B15)$$

$$I_N = (\beta_N + \gamma_N) \alpha_{N-1} (C_{N-1}^0 - d_{0,N-2} - \alpha_{N-1} C_{N-2}^0). \quad (B16)$$

The functions,  $I_j$ , occur in the polynomials resulting from applying derivatives to  $\exp(iD(A)/C)$  in Appendix C.

Finally we note that the following identities may be proved from eqns. (B.2) and (B.3):

$$C_j^i = (\alpha_i + \alpha_{i+1} + \beta_{i+1} + \gamma_{i+1}) C_j^{i+1} - \alpha_{i+1}^2 C_j^{i+2} \quad (B17)$$



$$c_j^i = (\alpha_{j-1} + \alpha_j + \beta_j + \gamma_j) \, c_{j-1}^i - \alpha_{j-1}^2 \, c_{j-2}^i \quad (\text{B18})$$

### Appendix C. The Derivatives of $\exp(iD(A)/C)$

We compute the derivatives with respect to  $A_i (i=0, \dots, N)$  of  $\exp(\frac{iD(A)}{C})$  in this section where  $D(A)$  is given by eq. (A6). Let

$$Z_j(j(A))_v = (A_j - A_0 - q)_v G_j + (A_j + p)_v H_j + \sum_{r=1}^N (A_j - A_r) I_{rj} + (q + p + A_0)_v G$$

with  $Z_j = (\beta_j + \gamma_j)$ ,  $I_{rj} = I_{jr}$ ,  $I_{rr} = 0$  and other quantities defined as in eq. (A6). Then

$$\frac{\partial}{\partial A_j^v} \exp\left(\frac{iD(A)}{C}\right) = \frac{2iZ_j(j(A))_v}{C} \exp\left(\frac{iD(A)}{C}\right)$$

The application of further derivatives will be complicated by the  $A$  dependence of  $(j(A))_v$ . To deal with this additional complexity we define

$$\frac{\partial}{\partial A_k^\mu} (j(A))_v = Z_k(kj)_{\mu v}$$

and

$$(j(A))_v \Big|_{A_0=A_1=\dots=A_N=0} = (j)_v = \frac{p_v H_j - q_v G_j}{Z_j}$$

Therefore if  $j, k \in \{1, 2, \dots, N\}$  then

$$Z_j Z_k(kj) = \delta_{jk} (G_j + H_j + I_j) - I_{kj}$$

with  $\delta_{jk}$  a Kronecker delta,  $(kj) = (jk)$ , and  $I_j$  given in eq. (B.14). Some particular cases of interest are

$$(i)_v = p_v d_{iN} C_{i-1}^0 - q_v d_{0i-1} C_N^i \quad i = 1, 2, \dots, N \quad (C1)$$

$$(0)_v = p_v d_{1N} + q_v C' \quad (C2)$$

$$(ij) = -d_{ij-1} C_{i-1}^0 C_N^j \quad i < j; i, j = 1, 2, \dots, N \quad (C3)$$

$$(0i) = -d_{1i-1} C_N^i \quad i = 2, 3, \dots, N \quad (C4)$$

$$(01) = -C_N^1 \quad (C5)$$

$$(ii) = \frac{\alpha_{i-1} C_N^i (C_{i-1}^0 - \alpha_{i-1} C_{i-2}^0) + \alpha_i C_{i-1}^0 (C_N^i - \alpha_i C_N^{i+1})}{\beta_i + \gamma_i} \quad i = 2, 3, \dots, (N-1) \quad (C6)$$

$$(11) = \frac{(\alpha_0 + \alpha_1) C_N^1 - \alpha_1^2 C_N^2}{\beta_1 + \gamma_1} \quad (C7)$$

$$(NN) = \frac{(\alpha_N + \alpha_{N-1}) C_{N-1}^0 - \alpha_{N-1}^2 C_{N-2}^0}{\beta_N + \gamma_N} \quad (C8)$$

These definitions will enable us to calculate the derivatives of  $\exp(\frac{iD(A)}{C})$  for the general case and write the result in a compact form. The following examples of second and fourth order derivatives illustrate the use of quantities defined above.

( $k_1, k_2, k_3$  and  $k_4$  are integers from the set  $\{0, 1, \dots, N\}$ ):

$$\left[ \frac{1}{Z_{k_1} Z_{k_2}} \frac{\partial^2}{\partial A_{k_2}^{v_2} \partial A_{k_1}^{v_1}} \exp\left(\frac{iD(A)}{C}\right) \right]_{A=0} = \left[ \frac{2i}{C} g_{v_1 v_2}(k_1 k_2) + \left(\frac{2i}{C}\right)^2 (k_1)_{v_1} (k_2)_{v_2} \right] \exp\left(\frac{iD}{C}\right)$$

$$\left[ \prod_{j=1}^4 \frac{1}{Z_{k_j}} \frac{\partial}{\partial A_{k_j}^{v_j}} \exp\left(\frac{iD(A)}{C}\right) \right]_{A=0} = \left[ \left(\frac{2i}{C}\right)^2 \{ g_{v_1 v_2}(k_1 k_2) g_{v_3 v_4}(k_3 k_4) \} \right]$$

$$\begin{aligned}
& + g_{v_1 v_3} (k_1 k_3) g_{v_2 v_4} (k_2 k_4) + g_{v_1 v_4} g_{v_2 v_3} (k_1 k_4) (k_2 k_3) \} + \\
& + \left(\frac{2i}{C}\right)^3 \{ g_{v_1 v_2} (k_1 k_2) (k_3)_{v_3} (k_4)_{v_4} + g_{v_1 v_3} (k_1 k_3) (k_2)_{v_2} (k_4)_{v_4} + \\
& + g_{v_1 v_4} (k_1 k_4) (k_2)_{v_2} (k_3)_{v_3} + g_{v_2 v_3} (k_2 k_3) (k_1)_{v_1} (k_4)_{v_4} + \\
& + g_{v_2 v_4} (k_2 k_4) (k_1)_{v_1} (k_3)_{v_3} + g_{v_3 v_4} (k_3 k_4) (k_1)_{v_1} (k_2)_{v_2} \} + \\
& + \left(\frac{2i}{C}\right)^4 (k_1)_{v_1} (k_2)_{v_2} (k_3)_{v_3} (k_4)_{v_4} ] \exp \left(\frac{iD}{C}\right)
\end{aligned}$$

with  $Z_i = \beta_i + \gamma_i$  ( and  $Z_0 = \alpha_0$ ). It is clear from these examples that the terms in the coefficient of each  $\left(\frac{2i}{C}\right)^n$  are isomorphic to the perturbations in a certain class of the symmetric group. Thus  $g_{v_1 v_2} (k_1 k_2) g_{v_3 v_4} (k_3 k_4)$  corresponds to the permutation (12) (34), and  $g_{v_1 v_2} (k_1 k_2) (k_3)_{v_3} (k_4)_{v_4}$  to (12). This isomorphism gives us an algorithm for determining the coefficient of  $\left(\frac{2i}{C}\right)^n$  from the appropriate corresponding class in the symmetric groups. As a result the fourth order derivative expression may be rewritten

$$\left(\frac{2i}{C}\right)^2 \{2^2\} + \left(\frac{2i}{C}\right)^3 \{21^2\} + \left(\frac{2i}{C}\right)^4 \{1^4\}$$

with the terms corresponding to each bracket easily determined from the class of  $S_4$  (the symmetric group on four objects) having the cycle structure given in the bracket.<sup>27</sup>

The general case of the  $p^{\text{th}}$  order derivative operating on  $\exp(iD(A)/C)$  is given by

$$\begin{aligned}
\left[ \prod_{j=1}^p \frac{1}{Z_{k_j}} \frac{\partial}{\partial A_{k_j}} \right] \exp\left(\frac{iD(A)}{C}\right) \Big|_{A=0} &= \sum_{h_1+2h_2=p} \left(\frac{2i}{C}\right)^{h_1+h_2} \{2^{h_2} 1^{h_1}\} \\
&= \sum_{h=0}^{\left[\frac{p}{2}\right]} \left(\frac{2i}{C}\right)^{p-h} \{2^h 1^{p-2h}\} \quad (C9)
\end{aligned}$$

with  $[\frac{p}{2}]$  being the greatest integer less than  $\frac{p}{2}$  and the terms in  $\{2^{h_1 p - 2h}\}$  isomorphic to the permutations in the class of  $S_p$  with cycle structure  $2^{h_1 p - 2h}$ . With this expression for the  $p^{\text{th}}$  derivative we can proceed to evaluate the parts of these Feynman parameter polynomials which contribute to the leading behavior of the  $N+1$  rung diagram integral.

We now investigate the polynomial resulting from applying the derivative  $(0 < L_1 < L_2 \dots < L_m)$ ,

$$\frac{p^\lambda}{\alpha_0 \prod_{i=1}^m Z_{L_i}^2} \frac{\partial^{2m+1}}{\partial A_0^v \partial A_{L_1}^\mu \partial A_{L_1}^{v_1} \partial A_{L_2}^{v_1} \partial A_{L_2}^{v_2} \dots \partial A_{L_m}^{v_{m-1}} \partial A_{L_m}^\lambda},$$

to  $\exp(iD(A)/C)$ . This polynomial

$$\sum_{h=0}^m \left(\frac{2i}{C}\right)^{2m+1-h} \{2^{h_1 2m+1-2h}\},$$

will be shown to give the following contribution to the leading behavior of the  $p_\mu p_\nu$  part of  $T_{N\mu\nu}$ :

$$p_\mu p_\nu \sum_{h=0}^m \left(\frac{2i}{C}\right)^{2m+1-h} (-1)^m f(m,h) d_{1N}(d_{0N} p \cdot q)^{m-h} \prod_{i=1}^m C_{L_i}^0 C_N^{L_i} \quad (C10)$$

with  $f(m,h)$  an integer.

Since factors of  $\alpha_i$  in the numerator of the Feynman parameter integral suppress the leading behavior of the integral we wish to find the part of  $\{2^{h_1 2m+1-2h}\}$  with the minimum number of such factors. More precisely, given two terms in the polynomial count the number of powers of  $q \cdot p$  and  $q^2$  in each term and divide by  $d_{0N}$

raised to the respective power in each term. (Due to the variables in which we have chosen to find the asymptotic behavior of the Feynman integral, the integral's asymptotic behavior is unaffected by factors of  $q^2 d_{0N}$  or  $q.p d_{0N}$ ). The term now containing the least number of powers of  $\alpha_0$  is leading. Should they be the same then the term with the least number of different  $\alpha_i$  is leading, etc. These considerations imply the following rules: (i) if a factor of  $(L_i)_\alpha (L_j)^\alpha$  occurs in a term,  $i < j$ , then  $-q.p d_{0L_i-1} d_{L_j N} C_N^{L_i} C_{L_j-1}^0$  is the leading part of this factor; (ii) if  $(L_i)_\lambda$  occurs in a term then  $-q_\lambda d_{0L_i-1} C_N^{L_i}$  is the leading part of this factor; (iii) any term with  $(L_i L_i)$  as a factor is not a leading term since there are other terms in  $\{2^h 1^{2m+1-2h}\}$  in which the two  $L_i$  are in combinations contributing a  $q.p d_{0N}$  factor (for example) while in  $(L_i L_i)$  they contribute a factor of  $\alpha_{L_i}$  or  $\alpha_{L_i-1}$ ; (iv) for reasons similar to those given in (iii) terms with factors having the form  $(L_i L_j)(L_i L_k)$  or  $(L_j L_i)(L_k L_i)$  are also not leading. As a result of these rules we can calculate the leading parts given in the following examples:

$$\begin{aligned} \{1^{2m+1}\} &\rightarrow (-1)^m d_{1N} (p.q d_{0N})^m \prod_{i=1}^m C_{L_i-1}^0 C_N^{L_i} p_\mu p_\nu \\ \{21^{2m-1}\} &\rightarrow (-1)^m \binom{m+1}{2} d_{1N} (p.q d_{0N})^{m-1} \prod_{i=1}^m C_{L_i-1}^0 C_N^{L_i} p_\mu p_\nu \end{aligned}$$

where  $f(m,1) = \binom{m+1}{2}$  counts the number of leading terms in the second example which is the number of distinct choices (ab) where  $a < b$  and  $a, b \in \{0, L_1, L_2, \dots, L_m\}$ .

The leading part of the general term  $\{2^h 1^{2m+1-2h}\}$  is given by the  $h^{\text{th}}$  term in the sum of eq. (C10). The factor  $(p.q d_{0N})^{m-h}$  arises from  $2m+1-2h$   $(L_i)_\alpha (L_j)_\beta$  factors occurring in each term of this set. Due to rules (iii) and (iv) given above the number of leading terms,  $f(m,h)$  is the number of distinct objects,

$$(a_1 b_1) (a_2 b_2) \dots (a_h b_h) ,$$

which can be formed by all possible choices of  $a_i$  from the set  $\{0, 1, 2, \dots, m-1\}$  and  $b_i$  from the set  $\{1, 2, \dots, m-1, m\}$  such that  $a_i < b_i$ , no integer occurs twice in the set  $\{a_1, a_2, \dots, a_h\}$ , and no integer occurs twice in the set  $\{b_1, b_2, \dots, b_h\}$ . Two terms which are the same except for the ordering of the factors  $(a_j b_j)$  are not considered distinct.

A recurrence relation for  $f(m, h)$  can be easily derived. The number of objects formed above in which a factor  $(a_j m)$  occurs for some  $j$  is given by

$$f(m, h) - f(m-1, h).$$

We now consider how this set of objects containing a factor  $(a_j m)$  can be formed. One method would be to take the set of objects enumerated by  $f(m-1, h-1)$  whose general term is

$$(a_1 b_1) (a_2 b_2) \dots (a_{h-1} b_{h-1})$$

and to each term in that set add an additional factor  $(a_j m)$ . The possible choices for  $a_j$  are limited by the fact that  $h-1$  out of the  $m$  possibilities  $0, 1, 2, \dots, m-1$  have already been chosen. Thus there are  $m-(h-1)$  different choices for the  $(a_j m)$  factor which can be added to each term. Since this exhausts all possible distinct terms we have

$$f(m, h) - f(m-1, h) = (m+1-h) f(m-1, h-1). \quad (C11)$$

We now show that

$$d_m = \sum_{h=0}^m (-1)^h (m+1-h)! f(m, h) = 1. \quad (C12)$$

Since  $d_0 = d_1 = 1$  all we need prove is that  $d_m$  is independent of  $m$ . Consider

$$\begin{aligned}
 I &= d_m - d_{m-1} \\
 &= \sum_{h=0}^m (-1)^h (m+1-h)! [f(m-1, h) + (m+1-h)f(m-1, h-1)] - \sum_{h=0}^m (-1)^h (m-h)! f(m-1, h) \\
 &= \sum_{h=0}^{m-1} (-1)^h (m-h)(m-h)! f(m-1, h) + \sum_{h=1}^m (-1)^h (m+1-h)(m+1-h)! f(m-1, h-1) \\
 &= \sum_{h=0}^{m-1} (-1)^h (m-h)(m-h)! f(m-1, h) + \sum_{h'=0}^{m-1} (-1)^{h'+1} (m-h')(m-h')! f(m-1, h') = 0
 \end{aligned}$$

where we used the recurrence relation in the second equation, recombined terms in the third equation and let  $h' = h-1$  in the second sum of the fourth equation. (Note that  $f(m, -1) = f(m, m+1) = 0$ .)

Finally we determine the terms with leading behavior in the polynomial resulting from the derivative (which is the previous derivative with  $\mu$  and  $\nu$  summed),

$$\frac{p^\lambda}{\alpha_0 \Pi Z_{L_i}^2} \frac{\partial^{2m+1}}{\partial A_{0\mu} \partial A_{L_1}^\mu \partial A_{L_1}^{\nu 1} \partial A_{L_2 \nu_1} \dots \partial A_{L_m}^\lambda}$$

applied to  $\exp(iD(A)/C)$ . Since we are summing over  $\mu$  and  $\nu$  we are interested in a slightly different part of the polynomials than the previous case. In particular, we wish to find terms containing one more power of  $q \cdot p$  than of  $\alpha_0$  so that  $W_1$  will eventually scale (neglecting  $\ln|q^2|$  factors). The factor that



gives this extra power of  $p.q$  is the  $q_\mu C'$  part of  $(0)_\mu$ . Therefore the only terms contributing to leading order are those with a factor of  $(0)_\mu$ . The leading part of the polynomial is given by

$$\sum_{h=0}^{m-1} \left( \frac{2i}{c} \right)^{2m+1-h} (-1)^{m_{p.q} C'} (d_{0N^{p.q}})^{m-h} f_1(m,h) \prod_{i=1}^m C_{L_i-1}^0 C_N^{L_i} \quad (C13)$$

where the only differences from eq. (C10) are to change  $p_\mu d_{1N}$  to  $q_\mu C'$  and sum over  $\mu$  and  $v$ , and to delete the  $h = m$  term since it contains no contribution to leading order. The number of terms in  $\{ 2^h 1^{2m+1-2h} \}$  contributing to leading order is different from the previous case and as a result we must investigate  $f_1(m,h)$ . The integer,  $f_1(m,h)$ , counts the number of distinct objects

$$(a_1 b_1) (a_2 b_2) \dots (a_h b_h)$$

which can be formed with all possible choices of  $a_i$  from  $\{ 1, 2, \dots, m-1 \}$  and  $b_i$  from  $\{ 1, 2, \dots, m \}$  under the same conditions as those given for  $f(m,h)$ . The only difference between the two enumerations is  $a_i$  can not equal 0 here (corresponding to the requirement that we must have  $(0)_\mu$ ) and thus no  $(0L_i)$  factors occur in leading terms. The result is a small change in the derivation of the recurrence relation for  $f_1(m,h)$  which is otherwise identical to the derivation for  $f(m,h)$ . Due to the loss of 0 from the set  $a_j$  could be chosen from, there are now only  $m-1-(h-1)$  possible ways of constructing a distinct term of the form

$$(a_1 b_1) \dots (a_j m) \dots (a_h b_h)$$

from each term in the set enumerated by  $f_1(m-1, h-1)$ . Thus we

have the recurrence relation:

$$f_1(m,h)=f_1(m-1,h)+(m-h)f_1(m-1,h-1). \quad (C14)$$

Because of the boundary conditions,  $f_1(2,1)=f(1,1)=f(1,0)$ , and eq. (C14) it is clear that

$$f_1(m,h)=f(m-1,h).$$

Therefore

$$\begin{aligned} d'_m &= \sum_{h=0}^{m-1} (-1)^h (m-h)! f_1(m,h) \\ &= d_{m-1} = 1 \end{aligned}$$

by our previous calculation for  $d_m$ .

## BIBLIOGRAPHY

1. E.D. Bloom et al., Report No. SLAC-PUB-796, Sept. 1970 (unpublished).
2. S.J. Brodsky, T. Kinoshita and H. Terazawa Phys. Rev. Letters 25, 972 (1970).
3. S.Drell and J. Walecka, Ann. Phys. (N.Y.) 28, 18 (1964).
4. J.D. Bjorken, Phys. Rev. 179, 1547 (1969).
5. J. Bjorken and S. Drell, Relativistic Quantum Mechanics, (McGraw-Hill, Inc., New York, 1964), p. 283.
6. S. Drell, D. Levy and T. Yan, Phys. Rev. D1, 1035 (1970).
7. S. Chang and P. Fishbane, Phys. Rev. D2, 1084 (1970).
8. T. Trueman and T. Yao, Phys. Rev. 132, 2741 (1963).
9. H. Abarbanel, M. Goldberger and S. Treiman, Phys. Rev. Letters 22, 500 (1969).
10. G. Altarelli and H. Rubinstein, Phys. Rev. 187, 2111 (1969).
11. S. Drell, D. Levy and T. Yan Phys. Rev. Letters 22, 744 (1969).
12. Bateman Manuscript Project, Table of Integral Transforms, edited by A. Erdelyi (McGraw-Hill, New York, 1954) p. 371.
13. R.J. Eden, P.V. Landshoff, D. Olive and J. Polkinghorne, The Analytic S-Matrix (Cambridge U.P., New York, 1966), pp. 32-36.
14. Reference 12, pp. 151-155.
15. Reference 11, p. 312.
16. Reference 11, p. 308.

17. S. Adler and W. Tung, Phys. Rev. Letters 22, 978 (1969);  
R. Jackiw and G. Preparata, *ibid* 22, 975 (1969).
18. J. Bjorken and T.T. Wu, Phys. Rev. 130, 2566 (1963).
19. T. Appelquist and J. Primack, Phys. Rev. D1, 1144 (1970).
20. R. Jackiw, Ann. Phys. (N.Y.) 48, 292 (1968).
21. J. Riordan, Combinatorial Identities, (John Wiley, New York, 1968) p. 12.
22. Reference 21, p. 76.
23. L. Hand, Phys. Rev. 129, 1834 (1963).
24. T. Gaisser and J. Polkinghorne, Report No. DAMTP 70/21  
Cambridge U., 1970 (unpublished).
25. S. Choudhury and V. Varma, Report No. IC/70/73, Miramare-  
Trieste, 1970 (unpublished).
26. S. Drell, D. Levy and T. Yan, Phys. Rev. 187, 2159 (1969).
27. M. Hamermesh, Group Theory, (Addison-Wesley, Reading  
Mass., 1962) p. 25.

**End**